Glycerol-3-phosphate acyltransferase 2 is essential for normal spermatogenesis

Maria B. Garcia-Fabiani[1]#, Mauro A. Montanaro[1]#, Pablo Stringa[2], Ezequiel Lacunza[3], Elizabeth R. Cattaneo[1], Marianela Santana[1], Magali Pellon-Maison[1] and Maria R. Gonzalez-Baro[1]*

1 Instituto de Investigaciones Bioquímicas de La Plata "Rodolfo R. Brenner", Consejo Nacional de Investigaciones Científicas y Técnicas, Facultad de Ciencias Médicas, Universidad Nacional de La Plata, La Plata 1900, Argentina.

2 Laboratorio de Trasplante de Órganos, Facultad de Ciencias Médicas, Universidad Nacional de La Plata, La Plata 1900, Argentina.

3 Centro de Investigaciones Inmunológicas Básicas y Aplicadas, Facultad de Ciencias Médicas, Universidad Nacional de La Plata, La Plata 1900, Argentina.

 # MBGF and MAM contributed equally to this work.

* **To whom correspondence should be addressed: email mgbaro@med.unlp.edu.ar.**

ABSTRACT: Glycerol-3-phosphate acyltransferases (GPAT) catalyze the first and rate-limiting step in the de novo glycerolipid synthesis. The GPAT2 isoform differs from the other isoforms because its expression is restricted to male germ cells and cancer cells. It has been recently reported that GPAT2 expression in mouse testis fluctuates during sexual maturation and that it is regulated by epigenetic mechanisms in combination with vitamin A derivatives. Despite progress made in this field, information about GPAT2 role in the developing male germ cells remains unclear. The aim of this study was to confirm the hypothesis that GPAT2 is required for the normal physiology of testes and male germ cell maturation. The gene was silenced in vivo by inoculating lentiviral particles carrying the sequence of a short-hairpin RNA targeting Gpat2 mRNA into mouse testis. Histological and gene expression analysis showed impaired spermatogenesis and arrest at the pachytene stage. Defects in reproductive fitness were also observed, and the analysis of apoptosis-related gene expression demonstrated the activation of apoptosis in Gpat2-silenced germ cells. These findings indicate that GPAT2 protein is necessary for the normal development of male gonocytes, and that its absence triggers apoptotic mechanisms, thereby decreasing the number of dividing germ cells.

SUMMARY STATEMENT

The product of the Gpat2 gene is highly expressed in testis. In vivo Gpat2 silencing in testis arrested spermatogenesis before the pachytene stage, increasing the expression of apoptosis-related genes.

SHORT TITLE

GPAT2 is required for spermatogenesis

KEYWORDS

Meiosis, apoptosis, mouse, gene silencing, germ cell, GPAT2

ABBREVIATIONS

GPAT: Glycerol-3-phosphate acyltransferase

KD: knock-down

KO: knock-out

shRNA: short-hairpin RNA

CT: cancer-testis

TAG: triacylglycerol

WT: wild type

RA: retinoic acid

FBS: fetal-bovine serum

Dpp: Days post-partum

FC: fold-change

FULL TEXT OF THE PAPER

Introduction

Glycerol-3-phosphate acyltransferases (GPAT) catalyze the first and rate-limiting step in *de novo* glycerolipid synthesis: the acylation of glycerol-3-phosphate with an acyl-CoA. Four isoforms,

product of different genes, have been identified in mammalian cells, the mitochondrial GPAT1 and GPAT2 and the endoplasmic reticulum GPAT3 and GPAT4 [1]. GPAT2 was first detected in liver mitochondria from *Gpat1 -/-* mice with an antibody raised against GPAT1 [2], and the mouse gene was then cloned based on sequence homology to *Gpat1 [3]*. Although it is highly similar to GPAT1 in its subcellular location, structure and sequence, GPAT2 has several characteristics that distinguish it from the other isoforms. GPAT1, GPAT3 and GPAT4 are expressed in lipogenic tissues and their activities are primarily associated with triacylglycerol (TAG) and phospholipid synthesis, using saturated and monounsaturated acyl-CoA as their major substrates. In contrast, GPAT2 is highly expressed in testis [3], and the overexpressed protein specifically esterifies arachidonoyl-CoA to both glycerol-3-phosphate and to 1-acylglycerol-3-phosphate [4]. Moreover, GPAT2 does not functionally substitute GPAT1, since compared to WT mice, *Gpat1 -/-* mice have reduced weight, lower content of liver TAG, and altered glycerolipid fatty acid composition [5]. In addition, *Gpat2* mRNA expression is neither regulated by the nutritional status of the animals [3] nor induced when 3T3-L1 fibroblasts differentiate into adipocytes [6]. Human GPAT2 is also ectopically expressed in some cancers and promotes a malignant phenotype [7]. These tissue-expression features together with the influence of GPAT2 on tumor progression led to the classification of this gene as a member of the Cancer Testis (CT) family, a group of genes expressed almost exclusively in normal testis and some tumors, which is important at specific stages of spermatogenesis [7,8]. CT genes are pathologically overexpressed in cancers of different origins and generally contribute to tumorigenesis and metastasis, which make them promising targets for directed immunotherapy [9]. In short, the testis expresses many of the oncogenes that are usually restricted to cancer cells [8].

Spermatogenesis is a complex developmental process during which spermatogonial stem cells divide, differentiate, and ultimately give rise to haploid spermatozoa. These processes occur within the seminiferous tubules which contain germ cells and Sertoli cells that create a microenvironment that sustains the generation of spermatozoa. This process can be divided into three phases: mitotic, meiotic, and spermiogenesis during which haploid round spermatids elongate and are released into the lumen of the seminiferous tubules as spermatozoa [10]. To achieve precise homeostasis in the adult, germ cell renewal, proliferation, export, and apoptosis must be finely balanced, a process that appears to occur at the cost of substantial germ cell wastage; as much as 75% of potential spermatozoa degenerate in the testes of adult mammals. Because Sertoli cells can only support a limited number of developing germ cells, the number of Sertoli cells present in adults determines the daily gamete production and apoptosis [11,12]. Additionally, spermatogenesis is strictly regulated and, in general terms, depends on the synchronized action of the hypothalamic-pituitary-gonadal axis and on epigenetics and small non-coding RNAs action [13,14,15].

Gpat2 expression in mouse testis is maximal at the pachytene stage, and its transcription is regulated by epigenetic mechanisms in combination with retinoic acid (RA) [6]. In addition, GPAT2 is required for piRNA biogenesis (16). PiRNAs are highly expressed in male germ cells and have broad functions in germline development, including transposon silencing and epigenetic

regulation [16,17,18]. Their name refers to Piwi-interacting RNA due to their relationship with members of the PIWI protein subfamily, such as the murine homologs MIWI, MILI and MIWI2. Based on their stage-specific expression, mammalian piRNAs can be classified into three groups: fetal, post-natal pre-pachytene, and pachytene piRNAs [19]. The first two groups are enriched in transposon sequences, coexpressed with MIWI2 and/or MILI in early stages of spermatogenesis, are primarily involved in *de novo* DNA methylation in fetal and perinatal male germ cells, and control retrotransposon expression [20]. Pachytene piRNAs, which are massively induced primarily from nontransposon intergenic regions in pachytene spermatocytes and post meiotic spermatids, generally do not target transposons, and their precise function is unknown [20]. These piRNAs are produced by primary processing, and GPAT2 is required for primary piRNA biogenesis [16]. Pachytene piRNAs are responsible for eliminating bulk mRNAs in spermatids during spermiogenesis, but are not always directly involved in the control of retrotransposon expression [20,21]. The mechanism by which GPAT2 promotes piRNA production remains unknown, but because promotion occurs in the absence of the acyltransferase motif $H(X_4)D$, regulation of piRNA production by GPAT2 is unlikely to require acyltransferase enzymatic activity [16]. The importance of PIWI proteins for the normal progression of spermatogenesis has been extensively documented and in mouse knock-out (KO) models, spermatogenesis stops at different stages [22,23,24,25].

Because the role of GPAT2 in developing male germ cells remains unclear, we investigated the effect of *Gpat2* downregulation during normal male germ cell maturation. We silenced GPAT2 in vivo by inoculating mouse testis with lentiviral particles carrying a gene encoding a short-hairpin RNA (shRNA) that targeted *Gpat2* mRNA. We found that *Gpat2* expression is necessary for the normal development of male gonocytes and that its absence triggers apoptosis, thereby decreasing the number of dividing germ cells.

Materials and Methods

Animals, cell lines, culture conditions and ethics statement

Animal protocols were approved by the Institutional Animal Care and Use Committee (Approval Number T10-02-2013) of the School of Medical Sciences, National University of La Plata (UNLP). Male BALB/c mice were housed on a 12-h light/12-h dark cycle with free access to water and standard chow (Cargill). Before testis dissections, mice were euthanized in a CO_2 chamber.

Cells were purchased from ATCC and grown at 37 °C in a 5% CO_2 atmosphere with 98% relative humidity. HEK293 and HEK293T human-derived cell lines were maintained in Dulbecco's modified Eagle's medium (DMEM) (Gibco), supplemented with 10% FBS and antibiotics (50 units/ml penicillin and 50 µg/ml streptomycin).

Gpat2 shRNA selection

GIPZ vectors carrying a gene encoding a shRNA targeting *Gpat2* transcript (shRNA-*Gpat2*) or a sequence that does not silence any mouse gene (scrambled sequence, Control vector) were purchased from Thermo Scientific (Thermo Scientific Open Biosystems Expression Arrest GIPZ Lentiviral shRNAmir). Five different shRNA-*Gpat2* vectors were acquired in order to select the most effective one. To test the efficiency of the vectors on *Gpat2* silencing, HEK293 human cell line was co-transfected with 1 µg of mouse *Gpat2* expression vector (pcDNA3.1-*Gpat2*, as previously reported [4]) and 5 µg of one of the different shRNA-*Gpat2* vectors or the Control vector. Cell transfection was carried out with Lipofectamine 2000 (Invitrogen), using a 3:1 (v/w) Lipofectamine: DNA ratio, in a six-well plate. Thirty-six hours after transfection, cells were lysed and RNA was isolated with TRIzol Reagent (Invitrogen) according to the manufacturer's instructions. *Gpat2* relative expression was evaluated by qPCR, using human TATA-box binding protein (*TBP*) as housekeeping gene. Primer sequences, shRNA sequences and selection results, vector information, and maps can be found in Supplementary Information (Tables S1 and S2, Figures S1 and S4).

Cell fractioning and immunoblotting

To test *Gpat2* silencing at the protein level, HEK293 cells were co-transfected with the *Gpat2* expression plasmid and the shRNA-*Gpat2* vector or the Control vector as described above. Cells were then rinsed with ice cold PBS and scraped from the plate with ice cold buffer H (10 mM HEPES-KOH, pH 7.4, 0.25 M sucrose, 1 mM EDTA and 1 mM dithiothreitol) with 0.002% v/v protease inhibitor cocktail (general use, Sigma) 1:6 (w/v). Total cellular homogenate was obtained by 10 up-and-down strokes in a motorized Teflon-glass vessel. Samples of 100 µg were separated by 8 or 12% SDS PAGE, transferred to a polyvinylidene difluoride membrane (Bio-Rad Laboratories), and probed with a 1:500 dilution of anti-GPAT2 antibody [4] or with 1:5000 of anti-glyceraldehyde 3-phosphate dehydrogenase (GAPDH) antibody (Santa Cruz Biotechnology), as the loading control. Membranes were then washed extensively and probed with 1:5000 dilution of horseradish peroxidase-conjugated goat anti-rabbit IgG antibody (Thermo-Pierce). For chemiluminescent detection, membranes were incubated with Super Signal detection kit (Thermo-Pierce) (Supplementary Information, Figure S1, B).

Lentiviral Production

After selecting the most effective silencing vector, lentiviral particles carrying that vector or the Control one, were produced in HEK293T cells. Cells were seeded at 50% confluence in 100 mm plates and the calcium phosphate method was used to co-transfect the shRNA-*Gpat2* or the Control vector (20 µg) with both the VSV-G envelope-expressing plasmid pMD2.G (Addgene, 10 µg) and the packaging plasmid psPAX2 (Addgene, 20 µg). Six hours later, the medium was replaced with fresh DMEM 5 % FBS and, 24 hours later, the medium was collected and stored at 4 °C. This last step was repeated for each plate the next two days. For lentiviral concentration, pooled media was ultracentrifuged for 2.5 hours at 21000 rpm in a SW32 Ti rotor (Beckman Coulter); the pellet was resuspended in 200 µl of cold PBS and stored at 4 °C ON. The next day, lentiviral particles were resuspended by pipetting up and down 30 times and stored at -80 °C in 50

µl aliquots for up to a month before testis inoculation. Lentiviral titration was achieved by transducing HEK293T cells with serial dilutions of the lentiviral particles and counting the GFP expressing colonies under a fluorescent microscope three days later. If the multiplicity of infection was acceptable (~1x10^8 Transforming Units/ml), testis inoculation was performed.

Lentiviral Inoculation

Eleven-day-old mice were anesthetized with isoflurane in O_2 (5% for induction and 1% for maintenance), an incision was made in the abdomen, testes were pulled out from the abdominal cavity and both testes were injected. Testes were inoculated with 50 µl of lentiviral particles with Polybrene (8 µg/ml, Sigma) and the vital dye trypan blue (0.004 % w/v). The trypan blue stain allowed us to follow lentiviral infiltration across the seminiferous tubules. After inoculation, the incision was sutured with a Vicryl suture 8-0, a single postsurgical dose of Tramadol (10 mg/Kg) was administered for pain control, and mice were returned to their cages with a nursing female mouse (Supplementary Information, Figure S2 A). Mice were monitored daily to evaluate their growth and health. They were sacrificed one month later and testes were removed.

To test the injection method and the surgical procedure before lentiviral inoculation, a group of 4 animals of 11 dpp was inoculated with PBS/trypan blue (0.004 % w/v). Mice were monitored daily, paying special attention to testis descent. Ten days after inoculation, two mice were sacrificed and testes were removed for histological analysis. The other two mice were mated with two healthy females in order to test their reproductive capacity (Supplementary Information, Figure S2, B).

Haematoxylin-Eosin staining and immunohistochemistry (IHC) analysis

Immediately after removal, testes were submerged in Bouin's fixation solution for at least 24 hours. Then, they were included in paraffin blocks, cut in 4 µm sections, deparaffinized and stained. For haematoxylin-eosin staining, slides were incubated in haematoxylin (Biopack) for 10 minutes, then rinsed with tap water, incubated for 5 minutes in eosin (Biopack), and rinsed with 50 % ethanol. After dehydration, slides were mounted and observed under a white-light Olympus BX52 microscope.

To evaluate the presence of ORF1p (LINE1 derived protein), IAP Gag (IAP derived protein) and GPAT2 we performed an IHC and samples were processed as previously described [4]. Slides were counter-stained with haematoxylin to visualize the nuclei and analyzed on an Olympus BX52 microscope.

Reproductive performance test

Nine shRNA-*Gpat2* and five Control inoculated mice were each mated with two healthy 30-day-old females and kept in separated cages. Breeding began a month after the lentiviral testis inoculation, and the test lasted until each female had had three litters. Sexual behavior, litter size and latency to first litter were evaluated.

Germ cell purification

Germ cells were isolated from the testes of inoculated mice as described [26]. Cells were incubated overnight at 34 °C in 4 % CO_2 to allow Sertoli cells to adhere to the culture plate surface. The germ-cell-enriched supernatant was removed and centrifuged for 10 min at 800 g at room temperature. After centrifugation, RNA was purified from cells with TRIzol reagent (Invitrogen).

Analysis of mRNA transcription by qPCR

After TRIzol purification, RNA quality was determined by gel electrophoresis and 260/230 and 260/280 nm absorbance ratios. One µg of total RNA was used for cDNA synthesis employing the High Capacity Reverse Transcription Kit (Applied Biosystems). A 1:10 cDNA dilution was used for qPCR (quantitative real-time PCR) with iTaq Universal SYBR Green Supermix (BioRad). Primers were designed to amplify the following mouse genes: *Gpat2*, *Nanos3*, *Tmem30c*, *Tpn1*, *Casp4*, *Cflar*, *Tnfrsf1a*, *Rnf7*, *Birc3*, *Pak, L15utr, L1orf, IAPltr, IAPgag,* and the mouse housekeeping gene *Rpl13a* or the human housekeeping gene *TBP* (Supplementary Information, Table S1). The thermal profile was 95 °C for 1 min, followed by 40 cycles of 95 °C for 20 sec, 55 °C for 50 sec and 60 °C for 30 sec, on a Stratagene Mx3500P apparatus. RNA expression was quantified in duplicate using the ΔΔCT method, and each sample was normalized to the corresponding housekeeping gene using qBase software.

Mouse Apoptosis Array: to test the expression of genes related to the apoptosis cell signaling pathway, we employed a qPCR based RT2 Profiler Mouse Apoptosis PCR Array (SA Biosciences) designed to cross-examine the expression of groups of genes that are functionally and coordinately regulated. A 0.5 µg sample of RNA was used for cDNA synthesis, which employed DEPC-free, nuclease-free MiliQ water and a 1:5 dilution for qPCR. The thermal profile was 95 °C for 1 min, followed by 40 cycles of 95 °C for 20 sec and 60 °C for 90 sec, on a Stratagene Mx3500P apparatus. Raw data were analyzed by SA Bioscience's PCR Array Data Analysis Web Portal and relative levels of gene expression were normalized in all the samples to the expression levels of housekeeping genes (*Gusb*, *Hprt*, *Hsp90ab1*, *Gapdh* and *Actb*).

TAG quantity evaluation by thin layer chromatography (TLC)

Total lipids were extracted [27] from shRNA-*Gpat2* and Control testes and separated by TLC on silica-gel 60 plates (Merck), with a mobile phase composed of hexane - ethyl ether - acetic acid (80:20:2; v/v) for neutral lipids. All samples were chromatographed in parallel with pure TAG standard. To calculate TAG content, TLC was carbonized, scanned and analyzed with ImageJ software.

Statistics

Differences between the control and silenced cells or animals were analyzed by Student's t test or by Analysis of Variance (ANOVA) followed by Tukey´s HSD test. Results were considered significant at the 5% level.

Results

Lentiviral silencing of *Gpat2* arrests spermatogenesis at pachytene stage

We previously reported that *Gpat2* expression in rat and mouse is restricted to male germ cells, specifically to primary spermatocytes [4,6], and that expression varies in testis during intra-uterine development and postnatal maturation [6]. In mice, *Gpat2* mRNA expression peaks at 14-16 gestational days and at 15 days post-partum (dpp); its spatio-temporal expression correlates with piRNA synthesis [6]. To understand the role of GPAT2 in postnatal testis and to test the hypothesis that GPAT2 is necessary for normal spermatogenesis, its expression was silenced with lentiviral particles (Figure 1). Based on previous data from PIWI-KO mouse models [22,23,24,25] and considering the physical interaction between GPAT2 and MILI, it was hypothesized that in vivo *Gpat2* silencing would cause similar phenotypic alterations in spermatogenesis progression.

Before inoculation with lentiviruses, testis integrity and mouse survival were evaluated after PBS/trypan blue injection. Because mouse growth, survival and reproductive capacity were not affected after the procedure, we proceeded to inoculate mice with the lentiviral particles.

To overcome the blood-testis-barrier and to silence *Gpat2* only in this tissue, we inoculated lentiviral particles carrying a gene encoding a shRNA targeting *Gpat2* transcript or a scrambled sequence directly into the seminiferous tubules of 11 dpp mice (shRNA-*Gpat2* or Control mice, respectively). This age was selected because the testes are sufficiently developed to be easily manipulated, and postnatal *Gpat2* expression has not peaked yet (15 dpp) (Figure 1, B). At this precise point during the first wave of spermatogenesis (Figure 1,C), the *Gpat2* promoter region is completely demethylated, thus enabling its transcription [6].

Histological analysis of testes was carried out a month after lentiviral inoculation (41 dpp). WT testis sections of mice at this age (adult) show a variety of germ cells at different spermatogenic stages, including spermatogonia, spermatocytes, spermatids and spermatozoa [11,28,29] (Figure 1, D). In contrast, haematoxylin-eosin stained shRNA-*Gpat2* testis sections showed several seminiferous tubules with deficient spermatogenesis and germ cell maturation, and the absence of round spermatids or mature sperm cells (Figure 2). Despite these defects, the number of spermatogonia was not affected. Because our model is not a KO and lentivirus administration might not reach all the seminiferous tubules, we observed tubules with normal appearing spermatogenesis as well as tubules with impaired sperm maturation in the same slide of shRNA-*Gpat2* testis sections. Consistently, the proportion of affected tubules in the shRNA-*Gpat2* group (average: 49%) was significantly higher than those observed in the Control group (average: 10%) (Figure 2, C). These histological analyses revealed that *Gpat2* expression is essential for normal spermatogenesis.

IHC was carried out to correlate the absence of GPAT2 protein with defective spermatogenesis. In mouse testes inoculated with Control virus, normal histology was observed in all analyzed sections, confirming the presence of GPAT2 and its localization in pachytene cells (Figure 3, A). In contrast, the altered tubular histology in shRNA-*Gpat2* mouse testis sections correlated with the absence of a positive signal for GPAT2 protein (Figures 3, B and C). With the exception of a single sample (Figure 3, C), testes weight, size, and shape did not vary statistically between shRNA-*Gpat2* or Control animals (Figure 2, D).

To determine when spermatogenesis stops as a consequence of *Gpat2* silencing, the expression of spermatogenic stage-specific genes was evaluated by qPCR [30]. A significant decrease in *Gpat2* mRNA content in the shRNA-*Gpat2* group was confirmed (Figure 4, A) and the expression of meiosis-phase or cell-marker genes *Nanos3* (spermatogonia), *Tmem30* (pachytene spermatocytes) and *Tnp1* (spermatids) was then measured. No difference was observed in the expression of *Nanos3* between groups, whereas *Tmem30* and *Tnp1* expression was significantly lower in the shRNA-*Gpat2* group (Figure 4, B). Consistently, the proportion of decrease in *Gpat2* expression in shRNA-*Gpat2* germ cells (40%) was comparable to the proportion of decrease observed in the expression of the pachytene-cell marker gene, *Tmem30* (56 %).

***Gpat2* silencing affects reproductive capacity**

To correlate the histological and molecular consequences of *Gpat2* knock-down (KD) with biological outcomes, the effect of *Gpat2* silencing on male reproductive capacity was tested. ShRNA-*Gpat2* and Control mice were mated with WT females. Sexual behavior was normal and latency until the first litter did not vary between groups. The Control group had a statistically larger first litter compared to the shRNA-*Gpat2* group, but the differences disappeared in the next two litters (Figure 5, A). Compared to the histology one month after lentiviral inoculation, seminiferous tubules had recovered in both groups. The average percent of altered tubules was 26% in the shRNA-*Gpat2* group and 1.5% in the Control group (Figure 5, B, D and E). The proportion of affected tubules was still significantly higher in the shRNA-*Gpat2* group (18-fold higher damage than in the Control group), highlighting the importance of GPAT2 for the post-natal development of mouse testes. Testes weight and size remained similar between groups (Figure 5, C and S3).

The decrease in germ cell number in shRNA-*Gpat2* mice seminiferous tubules correlates with apoptosis activation, without retrotransposon derepression

The histological and reproductive consequences of shRNA-*Gpat2* mice motivated us to search for processes or pathways that might have been affected by the decrease in *Gpat2* expression. TAG synthesis was not affected, since the content of TAG did not vary significantly between Control and KD testes (Figure S5).

Because it was previously demonstrated that *Gpat2* KD impaired piRNA production in germ cells [16] and that piRNAs regulate the expression of retrotransposable elements [31], we evaluated the effect of *Gpat2* KD on retrotransposon expression. In shRNA-*Gpat2* and Control groups, no

significant differences were observed in the testicular mRNA content of LINE1 and IAP, two of the most active retrotransposons in mice [31], (Figure 6, A).

To determine whether the protein products of LINE1 (ORF1p) and IAP (IAP Gag) have a differential expression in germ cells, we performed IHC on testis slides one month after lentiviral inoculation and after the reproduction tests. These showed similar results. In both Control and shRNA-*Gpat2* testes, the ORF1p was detected in primary spermatocytes, as previously reported [32,33], (Figure 6, B). The IHC signal in shRNA-*Gpat2* normal tubules was also equal to that of Controls. The few germ cells remaining in the abnormal shRNA-*Gpat2* tubules frequently showed a robust positive signal for ORF1p. In contrast to ORF1p IHC, the signal of IAP Gag IHC was low and similar in both groups (Figure 6, C).

Because of the depleted cell number observed in shRNA-*Gpat2* mouse tubule sections, we assessed the expression profile of genes involved in apoptotic pathways. Using a 96 well based qPCR array, 86 apoptosis-related genes were measured, and their relative expression was analyzed. In shRNA-*Gpat2* germ cells, apoptosis-related gene expression was activated ($p<0.001$), with 12 genes significantly upregulated and 2 genes significantly downregulated (cut-off of $|Log_2$Fold-Change (FC)$|> 1$ or < 1, respectively) (Figure 7, A). The expression of several of these genes was confirmed by qPCR (Figure 7, B). To determine a preference for some apoptotic pathway, deregulated genes were classified by gene ontology nomenclature. This analysis revealed no association with any of general apoptotic pathways (extrinsic apoptotic signaling, intrinsic apoptotic signaling, extrinsic and intrinsic apoptotic signaling, and regulation of apoptotic process) (data not shown). However, according to Kegg 2016, considering genes with a FC> 1.3, a functional enrichment pathway analysis showed a significant association with apoptotic TNF and NF-kappa beta signaling pathways (Figure 7, C and Figure S6).

Discussion

This study reports for the first time the physiological relevance of GPAT2 expression in testis. We have shown that *Gpat2* depletion causes meiotic arrest, a reduction in reproductive fitness, and an upregulation of apoptotic pathway genes.

GPAT2 protein has particular characteristics that markedly distinguish it from other GPAT isoforms. On the one hand, this isoform is ectopically expressed in several types of human cancers and has been classified as a CT gene, not only for its tissue distribution, but also for its role in the development of a malignant phenotype [7]. On the other hand, GPAT2 is highly expressed in testis, where its localization is restricted to pachytene spermatocytes and where both epigenetic mechanisms and trans-acting factors regulate its transient expression [6]. Finally, although GPAT2 is required for piRNA biogenesis (16) and piRNA production is crucial for spermatogenesis [22,33,34], neither the role nor the importance of GPAT2 in testicular physiology has been evaluated.

We developed an in vivo model, in which *Gpat2* is silenced with lentiviral particles in a tissue-specific manner. This experimental design has several advantages. The phenotype is not as

extreme as might occur in a KO model in which prenatal and neonatal testis development would be affected. Further, because GPAT2 is not expressed in somatic testicular cells (i.e. Sertoli or Leydig cells) [4], silencing only affects the germ cell lineage.

Histologically, *Gpat2* silencing caused a significant depletion in germ cell number and failure to complete spermatogenesis in those tubules where GPAT2 protein was undetectable. When GPAT2 was absent, the architecture of testicular parenchyma was also deeply affected. Despite these findings, testis weight and size did not vary significantly between groups, probably because the viral particles did not reach all the tubules equally; however, in animals in which testicular architecture was severely damaged, the organ size was drastically reduced (Figure 3, C).

In combination with the striking histology and to identify the step in which spermatogenesis is interrupted in shRNA-*Gpat2* testes, qPCR was performed for cellular and spermatogenesis stage-specific genes. qPCR indicated downregulation of pachytene and spermatid specific genes in silenced germ cells, whereas no differences were found in spermatogonia-specific gene expression between groups, suggesting that *Gpat2* KD prevents germ cells from proceeding through the pachytene stage. The arrest at the pachytene stage correlates with the absence of spermatocytes beyond this stage in slides of shRNA-*Gpat2* testis. These observations are consistent with previous results showing that GPAT2 mRNA and protein are highly expressed precisely in pachytene spermatocytes [6].

In accordance with the histological damage observed in shRNA-*Gpat2* testes, Control mice had a larger first litter than the shRNA-*Gpat2* group. The fact that shRNA-*Gpat2* mice had tubules depleted in dividing germ cells strongly suggests a decrease in mature spermatozoa number that causes an alteration in the reproductive fitness. However, no differences were observed in the next two litters. This change probably occurred because lentiviral infection transduces a percentage of dividing cells but with constant cell replacement and differentiation, non-transduced germ cells might divide and replace the transduced ones, thus reestablishing the number of normally dividing cells and repaired reproductive capacity. Despite this possibility, *Gpat2* expression remained significantly lower in the shRNA-*Gpat2* group compared to the Control group even after the third litter (not shown). Another possibility is that if lentiviral inoculation did not reach all the tubules, the effect of *Gpat2* downregulation on reproductive fitness might be masked by the great quantity of sperm released in each ejaculation.

In order to further understand the role of GPAT2 in testicular physiology, and because GPAT2 protein is involved in piRNA biogenesis through its interaction with MILI (16), and Mili-/- germ cells fail to regulate LINE1 or IAP transposons [16,35,36], their expression was evaluated. No differences in IAP or LINE1 were found between Control and shRNA-*Gpat2* germ cells.

Retrotransposon deregulation and, particularly, LINE1 overexpression, has been largely associated with the ablation of piRNA-related proteins in mouse mutant models [31]. However, ORF1p protein, and the corresponding RNA, has also been found in WT testis. ORF1p expression during WT spermatogenesis has been detected in leptotene through mid-pachytene spermatocytes [33],

and in elongating spermatids and residual bodies, but not in spermatogonia, mature spermatozoa or Sertoli cells [32]. The results obtained after IHC are consistent with these reports. In both control and silenced mice, ORF1p protein was present in spermatocytes and spermatids. The fact that ORF1p in WT spermatocytes is found from leptotene until mid-pachytene stages agrees with the fact that, in shRNA-*Gpat2* animals, affected tubules show germ cells with a strong positive signal. Those positive shRNA-*Gpat2* spermatocytes could be leptotene-zigotene or even early-pachytene arrested spermatocytes that normally express ORF1p.

The role of transposon transient expression in meiosis is controversial. Transposon derepression would be dangerous to germ cell genomes, but strictly regulated short-term L1 expression might be a requisite or a consequence of the chromatin restructuration during meiosis. In fact, retrotransposon DNA sequences are linked to synaptonemal complex formation [33].

It appears that GPAT2 is necessary to reach or to complete the pachytene stage in which GPAT2 would interact with MILI to synthesize piRNAs by the primary pathway. While pre pachytene piRNAs are necessary for retrotransposon silencing, the precise function of postnatal pachytene piRNAs is not yet well understood [31]. One of their functions is to eliminate bulk mRNA during spermiogenesis [20]. Retrotransposon deregulation was first reported in KO mice with impaired piRNA synthesis from early embryonic stages [31]. However, postnatal disruption of piRNA production in testis may not modify LINE1 or IAP expression. For instance, MOV10L1 KO in postnatal mouse spermatocytes produces a specific loss of pachytene piRNAs without LINE1 and IAP derepression [37]. In fact, MOV10L1 co-precipitates with GPAT2 and MILI [16], suggesting that GPAT2 may function in a similar way. In accordance, pachytene piRNAs are produced by primary processing and, particularly, GPAT2 is required for primary piRNA biogenesis [16]. Thus, although GPAT2 has been linked to piRNA production through its interaction with MILI and its downregulation affects piRNA production, it is possible that it is not directly involved in the control of retrotransposon expression or, at least, in the expression of LINE1 and IAP transposons.

The canonical GPAT activity, the acylation of glycerol-3-phosphate, does not appear to be linked to the phenotype, since a) the final product of the pathway (TAG) did not change in silenced testes compared to controls, and b) *GPAT2* silencing by 80% in MDA-MB-231 cells did not affect GPAT enzymatic activity in vitro (Table S3). These data show that GPAT2 plays a role that is distinct from the synthesis of cellular glycerolipids. It is most likely that the striking phenotype is a consequence of impaired piRNA biogenesis and/or a critical signaling pathway. Consistent with the latter possibility, bioinformatics analysis showed that GPAT2 is the only mouse GPAT that contains intrinsically disordered protein regions [38], typical of scaffolding proteins in diverse signaling pathways [39,40] (Figure S6).

Because an increase in apoptosis might be the cause of germ cell depletion in *Gpat2* silenced seminiferous tubules, we evaluated the expression of 84 apoptosis-related genes in shRNA-*Gpat2* and Control derived germ cells. Twelve genes were significantly overexpressed in the shRNA-

Gpat2 group, and 2 genes were downregulated. The downregulated genes (*Pak* and *Rnf7*) are anti-apoptotic genes [41,42]. This statistically significant balance ($p<0.001$) is consistent with an enhancement of apoptotic pathways in *Gpat2* KD germ cells and, particularly TNF and NF-kappa beta (functioning as an activator of apoptosis [43]) pathways were the most upregulated ones.

The two major apoptotic pathways are the extrinsic or cell death receptor pathway and the intrinsic or mitochondrial pathway, but molecules involved in one pathway can influence the other. Apoptosis occurs primarily via the intrinsic pathway during fetal testis development and via the extrinsic pathway in postnatal germ cells [44]. Consistently, the receptors of the extrinsic pathway were among the most significantly upregulated genes in *Gpat2* KD germ cells (*Tnfrsf1a*, *Ltbr*, *Cd40* and *Fas,* Figure S7). In summary, these results combined with the observed histological consequences, support the conclusion that downregulating *Gpat2* results in the enhancement of intracellular apoptosis. It is not clear if apoptosis activation in *Gpat2* KD cells occurs as a secondary effect to the meiotic arrest after the activation of the "pachytene checkpoint" [45], or if GPAT2 is directly involved regulating apoptosis. Supporting the latter possibility, it was previously demonstrated that *GPAT2* silencing makes MDA-MB-231 breast cancer cells more sensitive to staurosporine induced apoptosis, whereas *GPAT2* overexpression makes cells more resistant to apoptosis [7].

Conclusion

In conclusion, this study reflects the importance of GPAT2 for the normal progression of spermatogenesis and the postnatal development of the testis. It also implies that GPAT2 regulates the activation of apoptotic pathways and is an essential protein for germ cell survival. Further experiments are needed to specify the exact molecular mechanisms by which GPAT2 influences apoptosis-related gene expression and promotes meiosis fulfillment.

Acknowledgements

We thank Mario Raul Ramos for the illustrations and Rodrigo Tarabini for the histological processing of samples. We are grateful to B. Cullen and A. Bortvin for IAP Gag and ORF1p antibodies. MAM, EL, MPM and MRGB are members of the Carrera del Investigador Científico y Tecnológico, and MBGF and PS are fellows of CONICET, Argentina.

Declarations of interest

The funders had no role in study design, data collection and analysis, decision to publish, or preparation of the manuscript.

Funding

This work was supported by PICT 3214 ANPCyT, PIP0310 CONICET and UNLP M168 (MRGB).

Author contribution

MRGB, MBGF, MM and MPM conceived and designed the experiments. MBGF, MM, PS, MS and EC performed the experiments. MBGF, MM, MRGB and EL analyzed the data. MRGB and EL contributed reagents/materials/analysis tools. MBGF, MM, MRGB and EL wrote the paper.

References

1. Wendel, A. A., Lewin, T. M. and Coleman, R. A. (2009) Glycerol-3-phosphate acyltransferases: rate limiting enzymes of triacylglycerol biosynthesis. Biochim. Biophys. Acta **1791**, 501-506

2. Lewin, T. M., Schwerbrock, N. M., Lee, D. P. and Coleman, R. A. (2004) Identification of a new glycerol-3-phosphate acyltransferase isoenzyme, mtGPAT2, in mitochondria. J. Biol. Chem. **279**, 13488-13495

3. Wang, S., Lee, D. P., Gong, N., Schwerbrock, N. M., Mashek, D. G., Gonzalez-Baro, M. R., Stapleton, C., Li, L. O., Lewin, T. M. and Coleman, R. A. (2007) Cloning and functional characterization of a novel mitochondrial N-ethylmaleimide-sensitive glycerol-3-phosphate acyltransferase (GPAT2). Arch. Biochem. Biophys. **465**, 347-358

4. Cattaneo, E. R., Pellon-Maison, M., Rabassa, M. E., Lacunza, E., Coleman, R. A. and Gonzalez-Baro, M. R. (2012) Glycerol-3-phosphate acyltransferase-2 is expressed in spermatic germ cells and incorporates arachidonic Acid into triacylglycerols. PLoS. One. **7**, e42986

5. Hammond, L. E., Gallagher, P. A., Wang, S., Hiller, S., Kluckman, K. D., Posey-Marcos, E. L., Maeda, N. and Coleman, R. A. (2002) Mitochondrial glycerol-3-phosphate acyltransferase-deficient mice have reduced weight and liver triacylglycerol content and altered glycerolipid fatty acid composition. Mol. Cell Biol **22**, 8204-8214

6. Garcia-Fabiani, M. B., Montanaro, M. A., Lacunza, E., Cattaneo, E. R., Coleman, R. A., Pellon-Maison, M. and Gonzalez-Baro, M. R. (2015) Methylation of the Gpat2 promoter regulates transient expression during mouse spermatogenesis. Biochem. J. **471**, 211-220

7. Pellon-Maison, M., Montanaro, M. A., Lacunza, E., Garcia-Fabiani, M. B., Soler-Gerino, M. C., Cattaneo, E. R., Quiroga, I. Y., Abba, M. C., Coleman, R. A. and Gonzalez-Baro, M. R. (2014) Glycerol-3-phosphte acyltransferase 2 behaves as a cancer testis gene and promotes growth and tumorigenicity in the breast cancer MDA-MB-231 cell line. PLoS. One. **9**, e100896

8. Cheng, Y. H., Wong, E. W. and Cheng, C. Y. (2011) Cancer/testis (CT) antigens, carcinogenesis and spermatogenesis. Spermatogenesis. **1**, 209-220

9. Ghafouri-Fard, S. and Modarressi, M. H. (2009) Cancer-testis antigens: potential targets for cancer immunotherapy. Arch. Iran Med. **12**, 395-404

10. Jan, S. Z., Hamer, G., Repping, S., de Rooij, D. G., van Pelt, A. M. and Vormer, T. L. (2012) Molecular control of rodent spermatogenesis. Biochim. Biophys. Acta **1822**, 1838-1850

11. Print, C. G. and Loveland, K. L. (2000) Germ cell suicide: new insights into apoptosis during spermatogenesis. Bioessays **22**, 423-430

12. Escott, G. M., da Rosa, L. A. and Loss, E. S. (2014) Mechanisms of hormonal regulation of sertoli cell development and proliferation: a key process for spermatogenesis. Curr. Mol. Pharmacol. **7**, 96-108

13. Hilz, S., Modzelewski, A. J., Cohen, P. E. and Grimson, A. (2016) The roles of microRNAs and siRNAs in mammalian spermatogenesis. Development **143**, 3061-3073

14. Rajender, S., Avery, K. and Agarwal, A. (2011) Epigenetics, spermatogenesis and male infertility. Mutat. Res. **727**, 62-71

15. Holdcraft, R. W. and Braun, R. E. (2004) Hormonal regulation of spermatogenesis. Int. J. Androl **27**, 335-342

16. Shiromoto, Y., Kuramochi-Miyagawa, S., Daiba, A., Chuma, S., Katanaya, A., Katsumata, A., Nishimura, K., Ohtaka, M., Nakanishi, M., Nakamura, T., Yoshinaga, K., Asada, N., Nakamura, S., Yasunaga, T., Kojima-Kita, K., Itou, D., Kimura, T. and Nakano, T. (2013) GPAT2, a mitochondrial outer membrane protein, in piRNA biogenesis in germline stem cells. RNA. **19**, 803-810

17. Beyret, E., Liu, N. and Lin, H. (2012) piRNA biogenesis during adult spermatogenesis in mice is independent of the ping-pong mechanism. Cell Res. **22**, 1429-1439

18. Aravin, A., Gaidatzis, D., Pfeffer, S., Lagos-Quintana, M., Landgraf, P., Iovino, N., Morris, P., Brownstein, M. J., Kuramochi-Miyagawa, S., Nakano, T., Chien, M., Russo, J. J., Ju, J., Sheridan, R., Sander, C., Zavolan, M. and Tuschl, T. (2006) A novel class of small RNAs bind to MILI protein in mouse testes. Nature **442**, 203-207

19. Luo, L. F., Hou, C. C. and Yang, W. X. (2016) Small non-coding RNAs and their associated proteins in spermatogenesis. Gene **578**, 141-157

20. Gou, L. T., Dai, P., Yang, J. H., Xue, Y., Hu, Y. P., Zhou, Y., Kang, J. Y., Wang, X., Li, H., Hua, M. M., Zhao, S., Hu, S. D., Wu, L. G., Shi, H. J., Li, Y., Fu, X. D., Qu, L. H., Wang, E. D. and Liu, M. F. (2014) Pachytene piRNAs instruct massive mRNA elimination during late spermiogenesis. Cell Res. **24**, 680-700

21. Siomi, M. C., Sato, K., Pezic, D. and Aravin, A. A. (2011) PIWI-interacting small RNAs: the vanguard of genome defence. Nat. Rev. Mol. Cell Biol. **12**, 246-258

22. Kuramochi-Miyagawa, S., Kimura, T., Ijiri, T. W., Isobe, T., Asada, N., Fujita, Y., Ikawa, M., Iwai, N., Okabe, M., Deng, W., Lin, H., Matsuda, Y. and Nakano, T. (2004) Mili, a mammalian member of piwi family gene, is essential for spermatogenesis. Development **131**, 839-849

23. Carmell, M. A., Girard, A., van de Kant, H. J., Bourc'his, D., Bestor, T. H., de Rooij, D. G. and Hannon, G. J. (2007) MIWI2 is essential for spermatogenesis and repression of transposons in the mouse male germline. Dev. Cell. **12**, 503-514

24. Deng, W. and Lin, H. (2002) miwi, a murine homolog of piwi, encodes a cytoplasmic protein essential for spermatogenesis. Dev. Cell **2**, 819-830

25. Vourekas, A., Zheng, Q., Alexiou, P., Maragkakis, M., Kirino, Y., Gregory, B. D. and Mourelatos, Z. (2012) Mili and Miwi target RNA repertoire reveals piRNA biogenesis and function of Miwi in spermiogenesis. Nat. Struct. Mol. Biol. **19**, 773-781

26. Boucheron, C. and Baxendale, V. (2012) Isolation and purification of murine male germ cells. Methods Mol. Biol. **825:59-66.**

27. Folch, J., Lees, M. and Sloane Stanley, G. H. (1957) A simple method for the isolation and purification of total lipides from animal tissues. J. Biol Chem. **226**, 497-509

28. Laiho, A., Kotaja, N., Gyenesei, A. and Sironen, A. (2013) Transcriptome profiling of the murine testis during the first wave of spermatogenesis. PLoS. One. **8**, e61558

29. Cheng, C. Y. and Mruk, D. D. (2012) The blood-testis barrier and its implications for male contraception. Pharmacol. Rev. **64**, 16-64

30. Hermo, L., Pelletier, R. M., Cyr, D. G. and Smith, C. E. (2010) Surfing the wave, cycle, life history, and genes/proteins expressed by testicular germ cells. Part 1: background to spermatogenesis, spermatogonia, and spermatocytes. Microsc. Res. Tech. **73**, 241-278

31. Chuma, S. and Nakano, T. (2013) piRNA and spermatogenesis in mice. Philos. Trans. R. Soc. Lond B Biol. Sci. **368**, 20110338

32. Branciforte, D. and Martin, S. L. (1994) Developmental and cell type specificity of LINE-1 expression in mouse testis: implications for transposition. Mol. Cell Biol. **14**, 2584-2592

33. van der Heijden, G. W. and Bortvin, A. (2009) Transient relaxation of transposon silencing at the onset of mammalian meiosis. Epigenetics. **4**, 76-79

34. Yadav, R. P. and Kotaja, N. (2014) Small RNAs in spermatogenesis. Mol. Cell Endocrinol. **382**, 498-508

35. Di, G. M., Comazzetto, S., Saini, H., De, F. S., Carrieri, C., Morgan, M., Vasiliauskaite, L., Benes, V., Enright, A. J. and O'Carroll, D. (2013) Multiple epigenetic mechanisms and the piRNA pathway enforce LINE1 silencing during adult spermatogenesis. Mol. Cell **50**, 601-608

36. Kuramochi-Miyagawa, S., Watanabe, T., Gotoh, K., Totoki, Y., Toyoda, A., Ikawa, M., Asada, N., Kojima, K., Yamaguchi, Y., Ijiri, T. W., Hata, K., Li, E., Matsuda, Y., Kimura, T., Okabe, M., Sakaki, Y., Sasaki, H. and Nakano, T. (2008) DNA methylation of retrotransposon genes is regulated by Piwi family members MILI and MIWI2 in murine fetal testes. Genes Dev. **22**, 908-917

37. Zheng, K. and Wang, P. J. (2012) Blockade of pachytene piRNA biogenesis reveals a novel requirement for maintaining post-meiotic germline genome integrity. PLoS. Genet. **8**, e1003038

38. Potenza, E., Di, D. T., Walsh, I. and Tosatto, S. C. (2015) MobiDB 2.0: an improved database of intrinsically disordered and mobile proteins. Nucleic Acids Res. **43**, D315-D320

39. Kjaergaard, M. and Kragelund, B. B. (2017) Functions of intrinsic disorder in transmembrane proteins. Cell Mol. Life Sci. doi: 10.1007/s00018-017-2562-5. [Epub ahead of print]

40. Uversky, V. N. (2015) The multifaceted roles of intrinsic disorder in protein complexes. FEBS Lett. **589**, 2498-2506

41. Wen, Y. Y., Zheng, J. N. and Pei, D. S. (2014) An oncogenic kinase: putting PAK5 forward. Expert. Opin. Ther. Targets. **18**, 807-815

42. Sun, Y. and Li, H. (2013) Functional characterization of SAG/RBX2/ROC2/RNF7, an antioxidant protein and an E3 ubiquitin ligase. Protein Cell **4**, 103-116

43. Sorriento, D., Illario, M., Finelli, R. and Iaccarino, G. (2012) To NFkappaB or not to NFkappaB: The Dilemma on How to Inhibit a Cancer Cell Fate Regulator. Transl. Med. UniSa. **4**, 73-85

44. Shaha, C., Tripathi, R. and Mishra, D. P. (2010) Male germ cell apoptosis: regulation and biology. Philos. Trans. R. Soc. Lond B Biol. Sci. **365**, 1501-1515

45. Roeder, G. S. and Bailis, J. M. (2000) The pachytene checkpoint. Trends Genet. **16**, 395-403

Figure 1

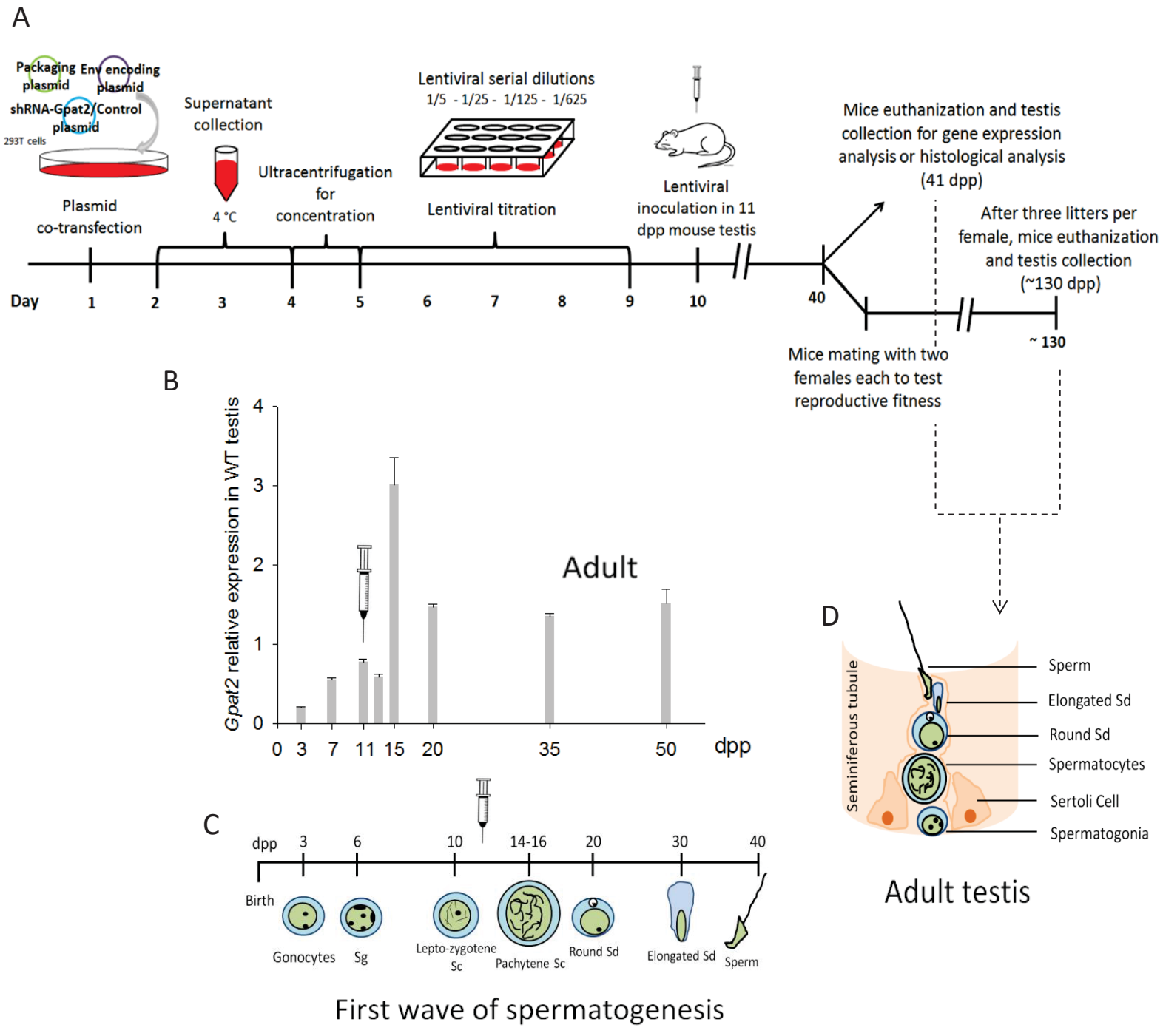

Figure 1. Experimental outline. (A) The timeline shows when lentivirus were produced, concentrated and injected into mice, and when testes were collected. (B) *Gpat2* relative expression during postnatal testis maturation in WT mice [6]. The syringe indicates *Gpat2*

expression when lentivirus are injected (11 dpp) and the word “Adult”, indicates the level of *Gpat2* expression in adult WT mouse testes. (C) A schematic timeline for the first wave of mouse spermatogenesis. The syringe indicates the stage of most germ cells when lentivirus are injected. (D) After the first wave, all stages of spermatogenesis can be observed in the adult mouse testes. Sg: spermatogonia, Sc: spermatocytes, Sd: spermatid.

Figure 2

A

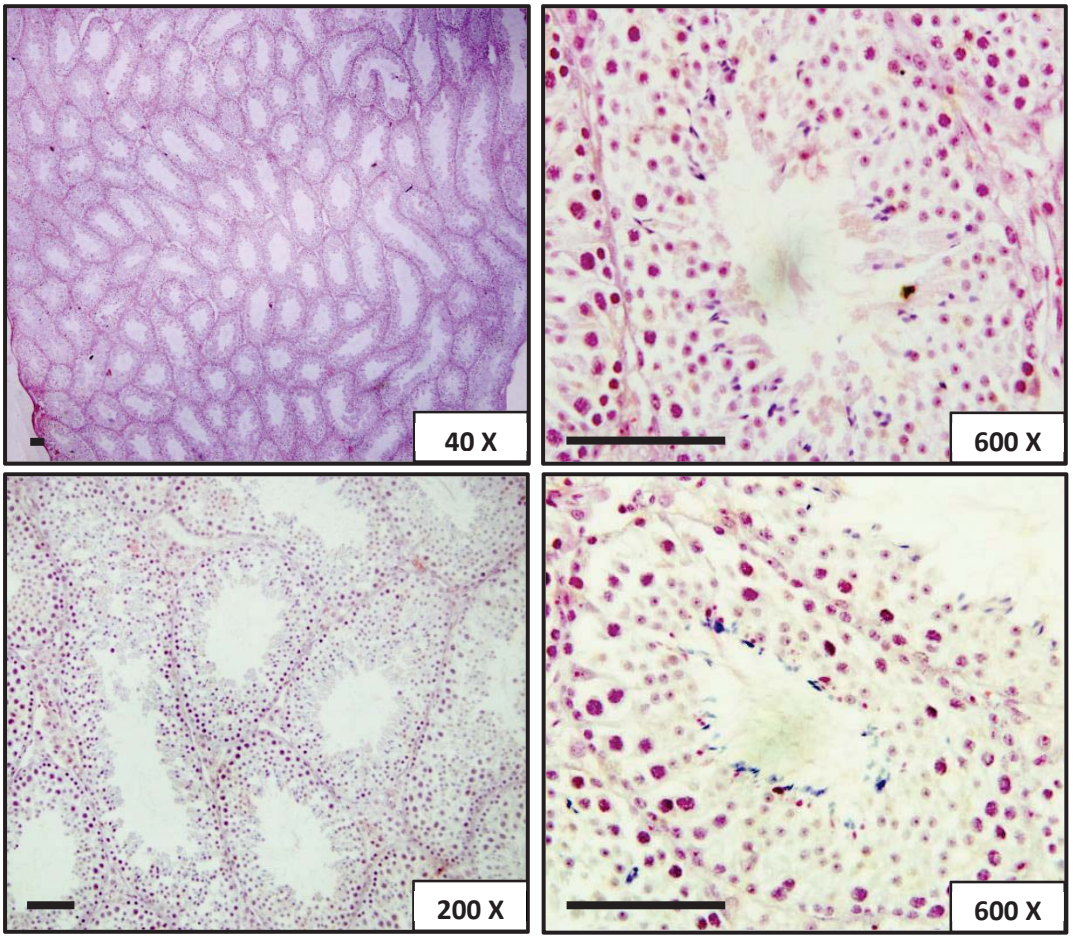

B

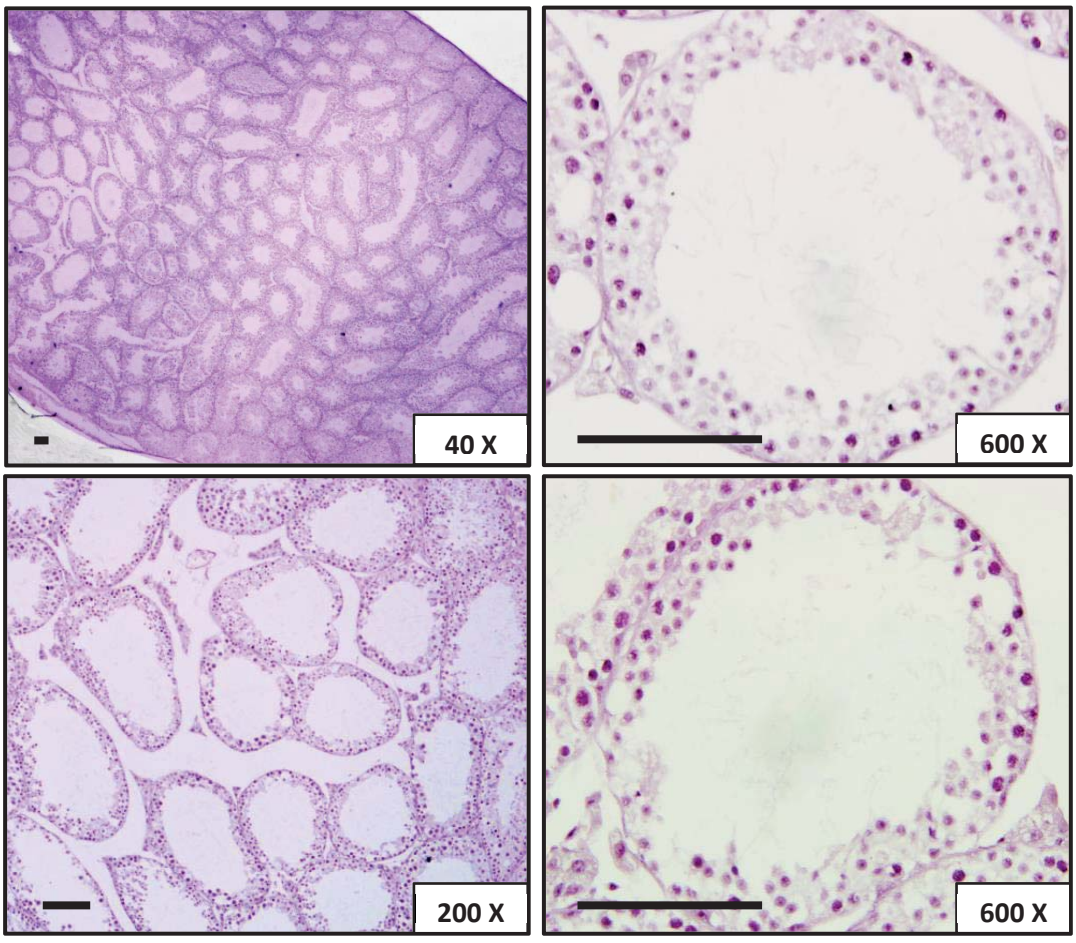

C

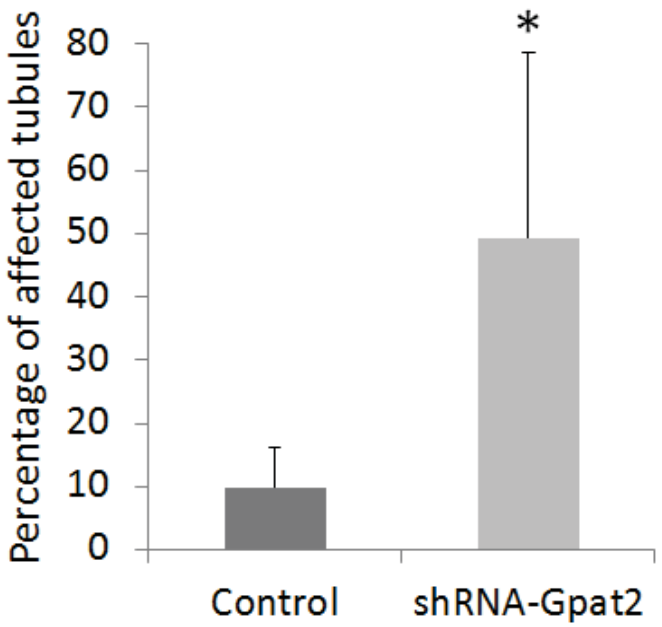

D

	Weight (g)
shRNA-*Gpat2*	0.092 ± 0.019
Control	0.1 ± 0.011

Figure 2. *Gpat2* silencing in mouse testis impairs spermatogenesis. Mouse testis were inoculated with (A) Control or (B) shRNA-*Gpat2* lentivirus in two independent experiments (n=4). Animals were sacrificed one month after the lentiviral inoculation. Slides were stained with haematoxylin-eosin. Six sections were analyzed from each animal. Pictures in A and B are representative and correspond to one sample testis from Control group or shRNA-*Gpat2* group, respectively. Magnifications are indicated in the lower right corner. Scale bars: 50 µm. (C) Percentage of affected seminiferous tubules ± SD. Student's T test, * $p<0.05$. (D) Testes weight was similar between groups.

Figure 3

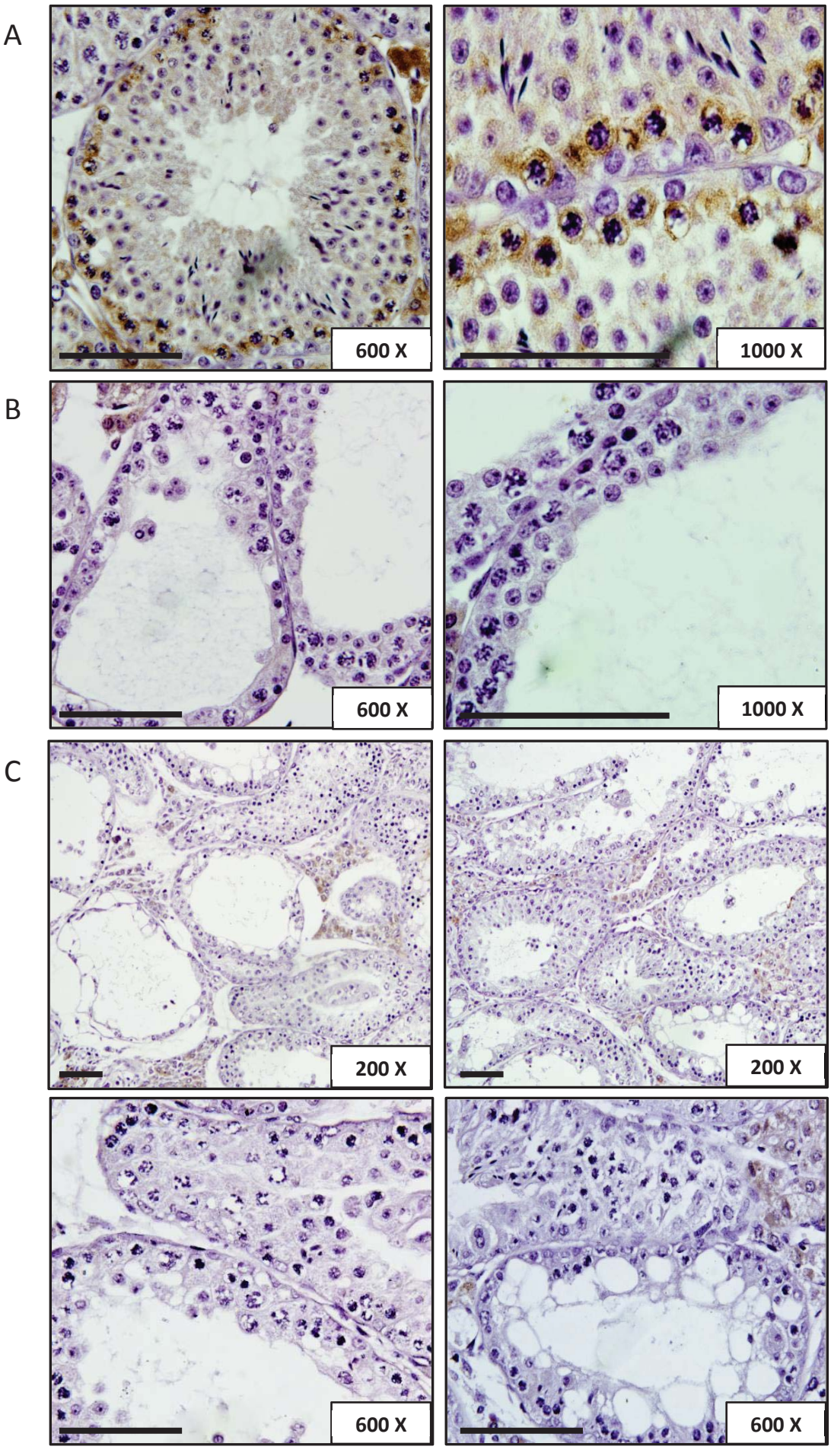

Figure 3. GPAT2 evaluation by IHC in *Gpat2* silenced or Control mouse testis. IHC was performed on slides from mouse testis inoculated with (A) Control or (B and C) shRNA-*Gpat2* lentivirus in two independent experiments (n=4). Animals were sacrificed one month after lentiviral inoculation. Six sections from each sample were analyzed. GPAT2 presence was detected by peroxidase reaction (brown stain) and nuclei were counterstained with haematoxylin (violet-blue stain). A representative testis section from one Control group animal (A) and two representative testis sections from two different shRNA-*Gpat2* animals (B and C) are shown. Magnifications are indicated in the lower right side of each image. Scale bars: 50 µM.

Figure 4

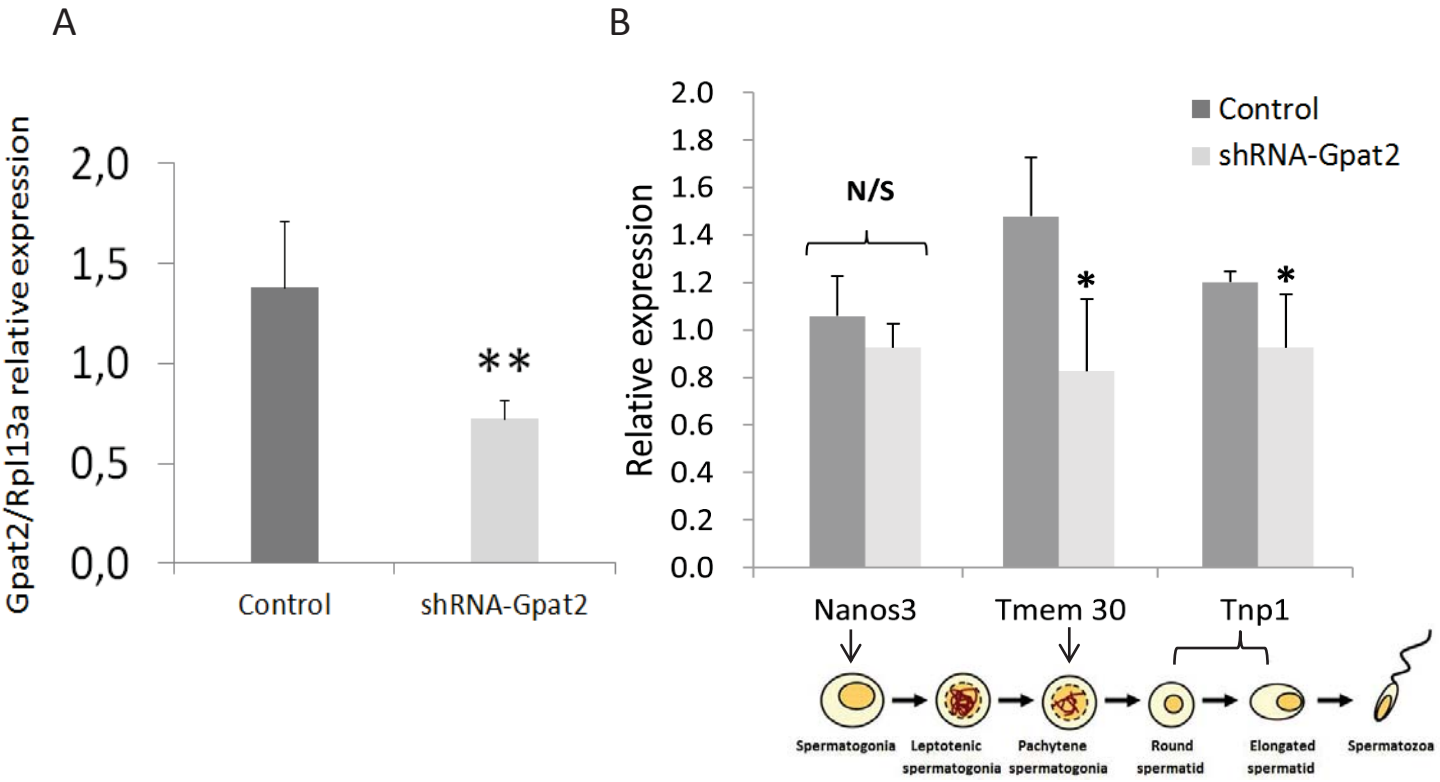

Figure 4. *Gpat2* silencing prevents germ cells from proceeding through the pachytene stage. (A) *Gpat2* and (B) spermatogenesis-stage or cell-specific gene expression was measured by qPCR, using *Rpl13a* as housekeeping gene. Under the histogram, a graphic

representation of spermatogenesis was included to show the stage at which each gene is predominantly expressed. Mean values ± SD from two independent experiments are shown. ** $p<0.01$; *$p<0.05$; N/S: no significant. Student's t test and ANOVA-Tukey HSD test.

Figure 5

A

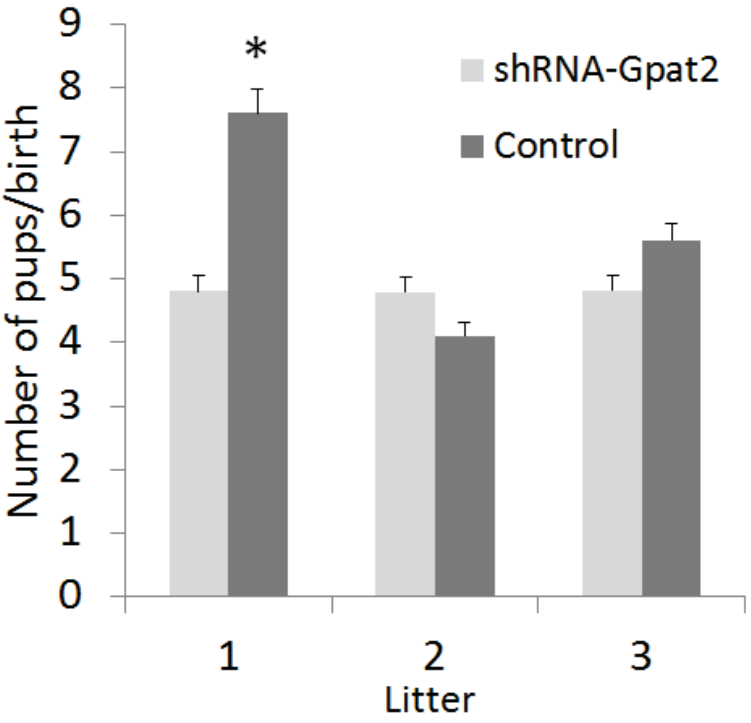

B

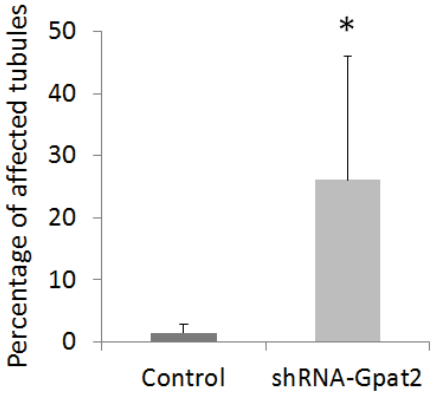

C

	Weight (g)
shRNA-*Gpat2*	0.1 ± 0.02
Control	0.095 ± 0.01

D

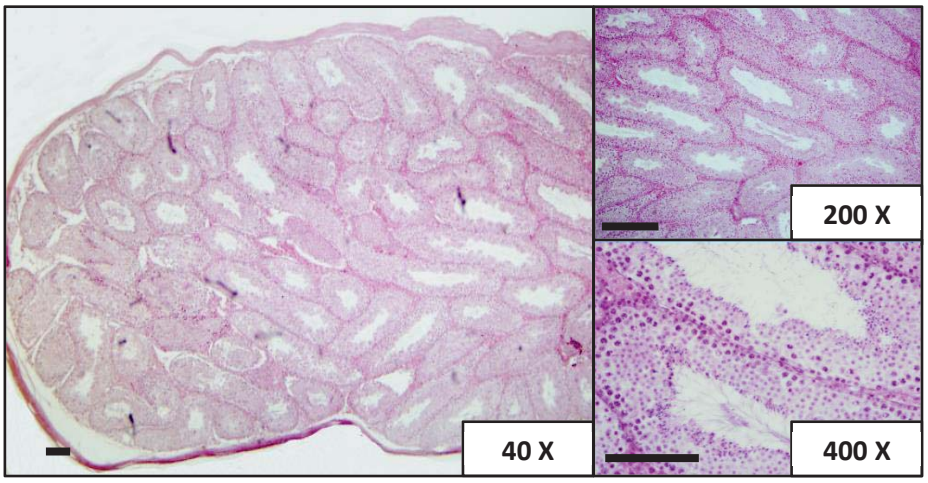

E

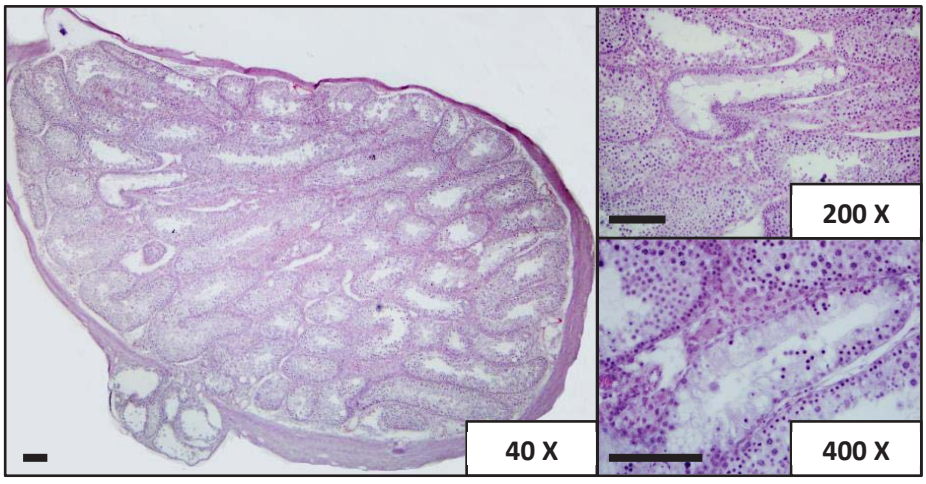

Figure 5. *Gpat2* silencing affects reproductive capacity. Nine or 5 mice were injected with shRNA-*Gpat2* or Control lentiviral particles, respectively. Each male was paired with two WT females. The experiment continued until each female had had three litters. (A) Average number of pups is shown per birth, per litter ± SD. Student's t test, *p<0.05. Mouse testicular sections were obtained after the reproductive capacity test in order to assess the degree of damage produced at 4 months after *Gpat2* silencing. (B) Average proportion of affected tubules of each group. (D and E) Representative slides from each group. Magnifications are shown at the lower right side of each image. Scale bars: 50 µM Student's t test, * p<0.05. (C) Testes weight was similar between groups.

Figure 6

A

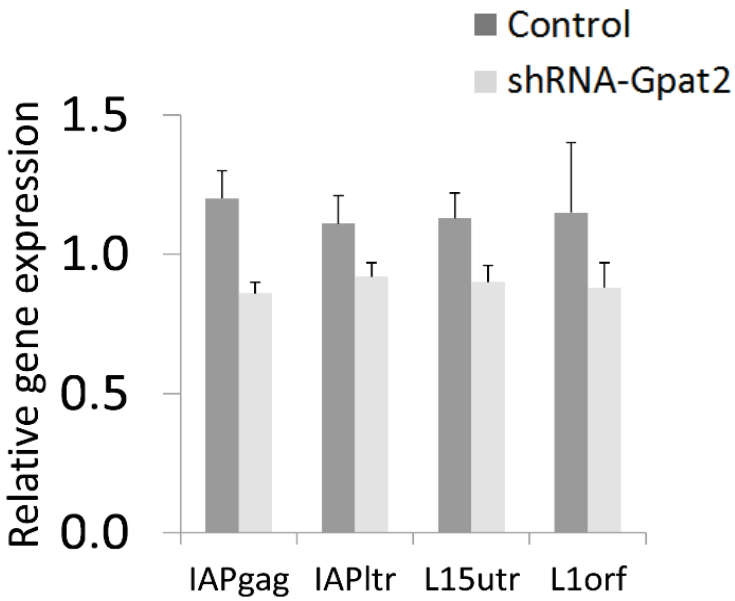
Control
shRNA-Gpat2
Relative gene expression
1.5
1.0
0.5
0.0
IAPgag
IAPltr
L15utr
L1orf

B

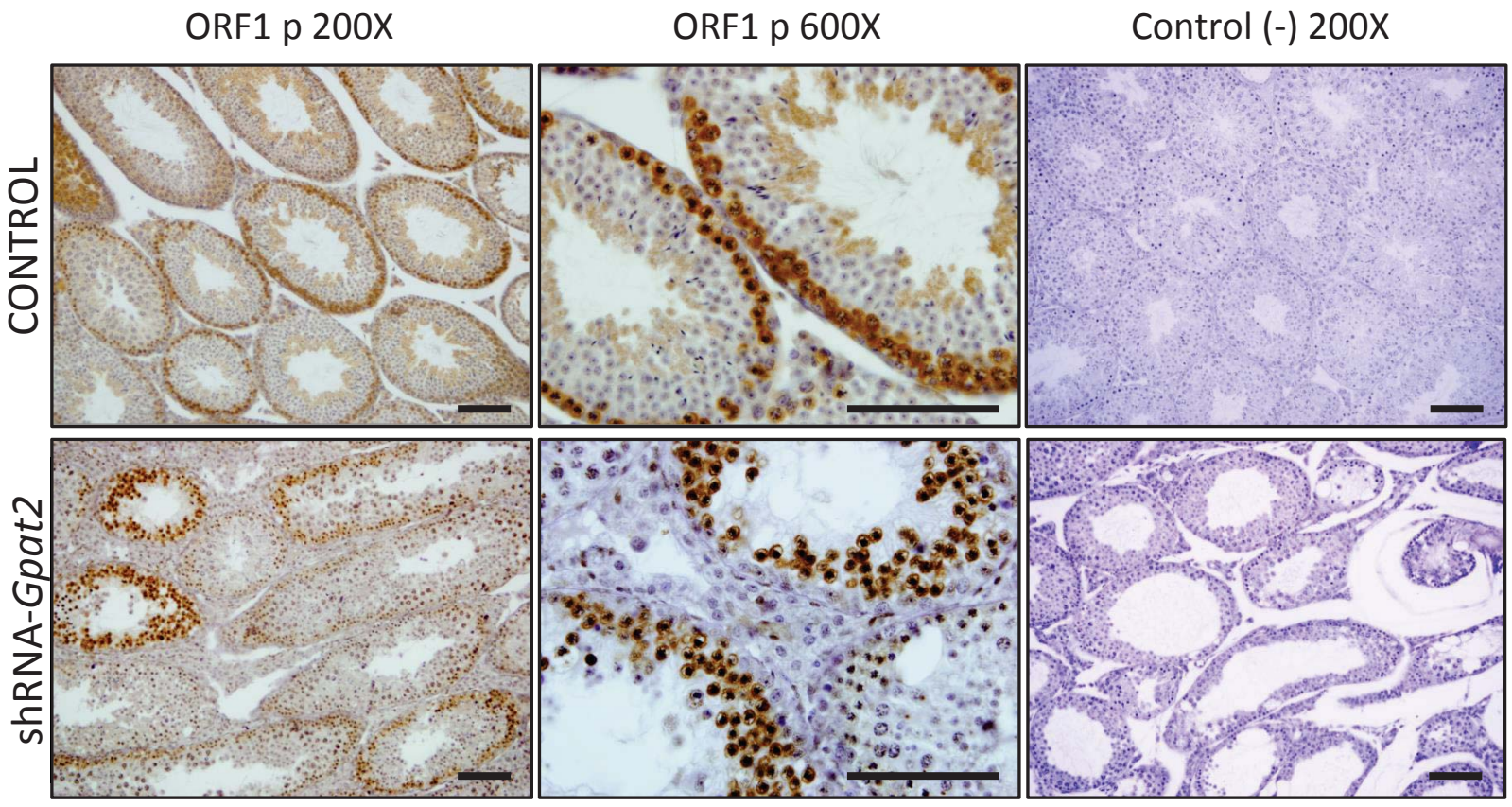
ORF1 p 200X
ORF1 p 600X
Control (-) 200X
CONTROL
shRNA-Gpat2

C

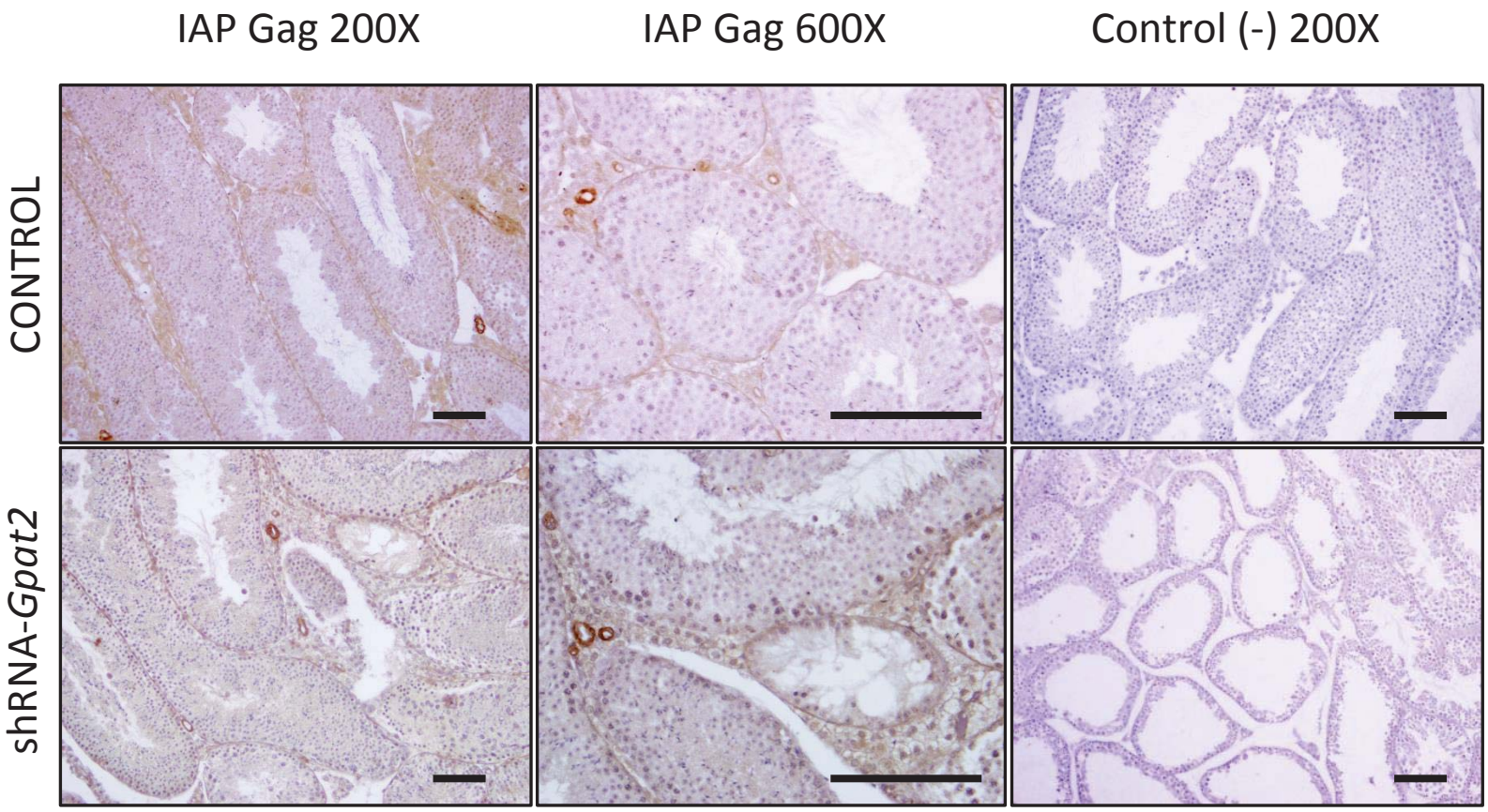

Figure 6. *Gpat2* silencing does not alter retrotransposon expression. (A) LINE1 and IAP mRNA expression was measured by qPCR, using *Rpl13a* as the housekeeping gene. Mice were inoculated with shRNA-*Gpat2* (n=7) or Control (n=5) lentiviral particles. After 30d germ cells were purified for RNA extraction. Mean values ± SD from two independent experiments are shown. No significant differences were detected between groups (ANOVA-Tukey HSD test). (B) LINE1-ORF1p was detected by IHC (brown stain) and nuclei were counterstained with haematoxylin (violet-blue stain). Negative control images are displayed in the third column. (C) IAP Gag IHC signal was not different between groups. Magnifications are indicated at the top of the columns. Scale bars: 50 µM.

Figure 7

A

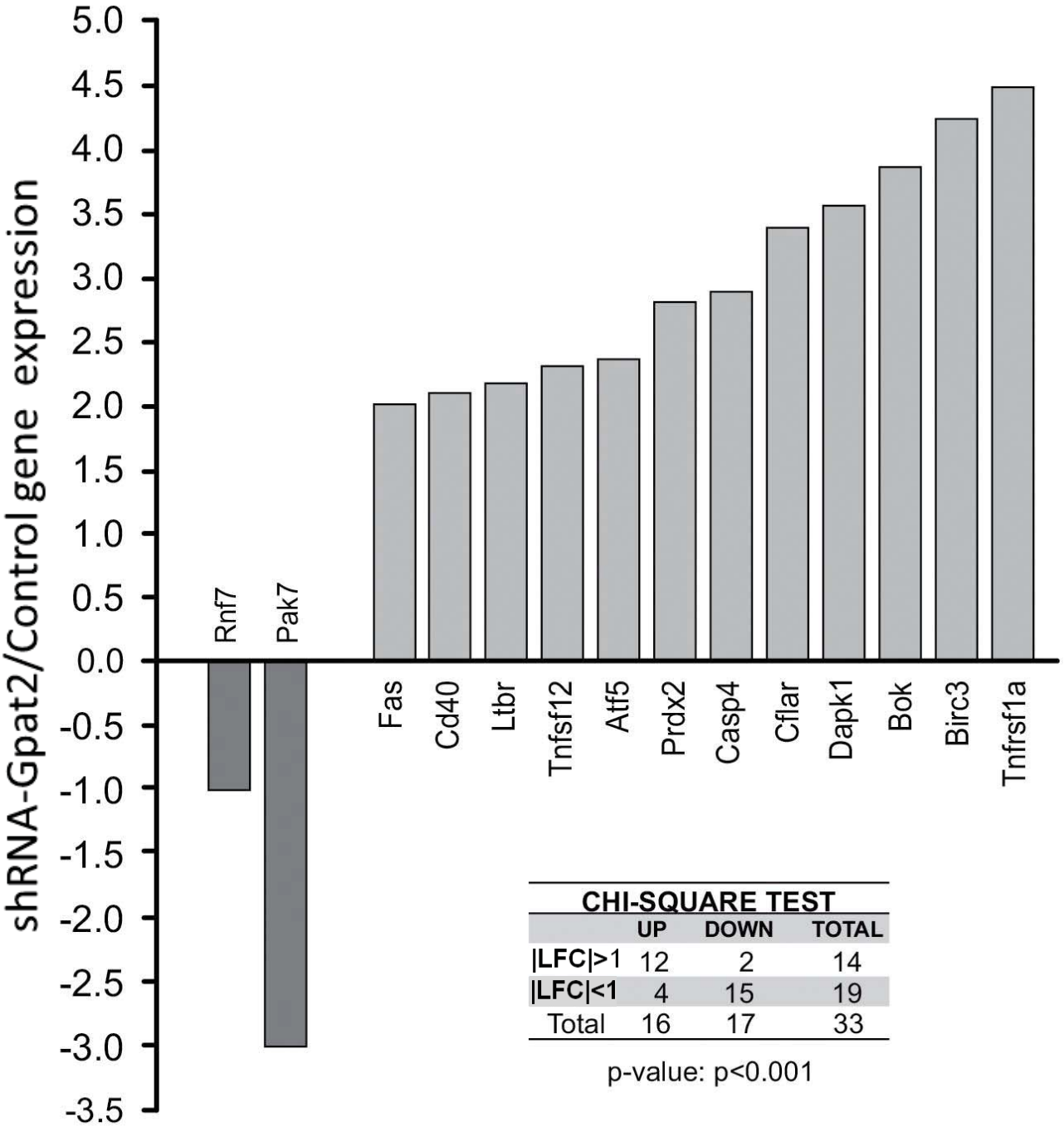

CHI-SQUARE TEST			
	UP	DOWN	TOTAL
|LFC|>1	12	2	14
|LFC|<1	4	15	19
Total	16	17	33

p-value: p<0.001

B

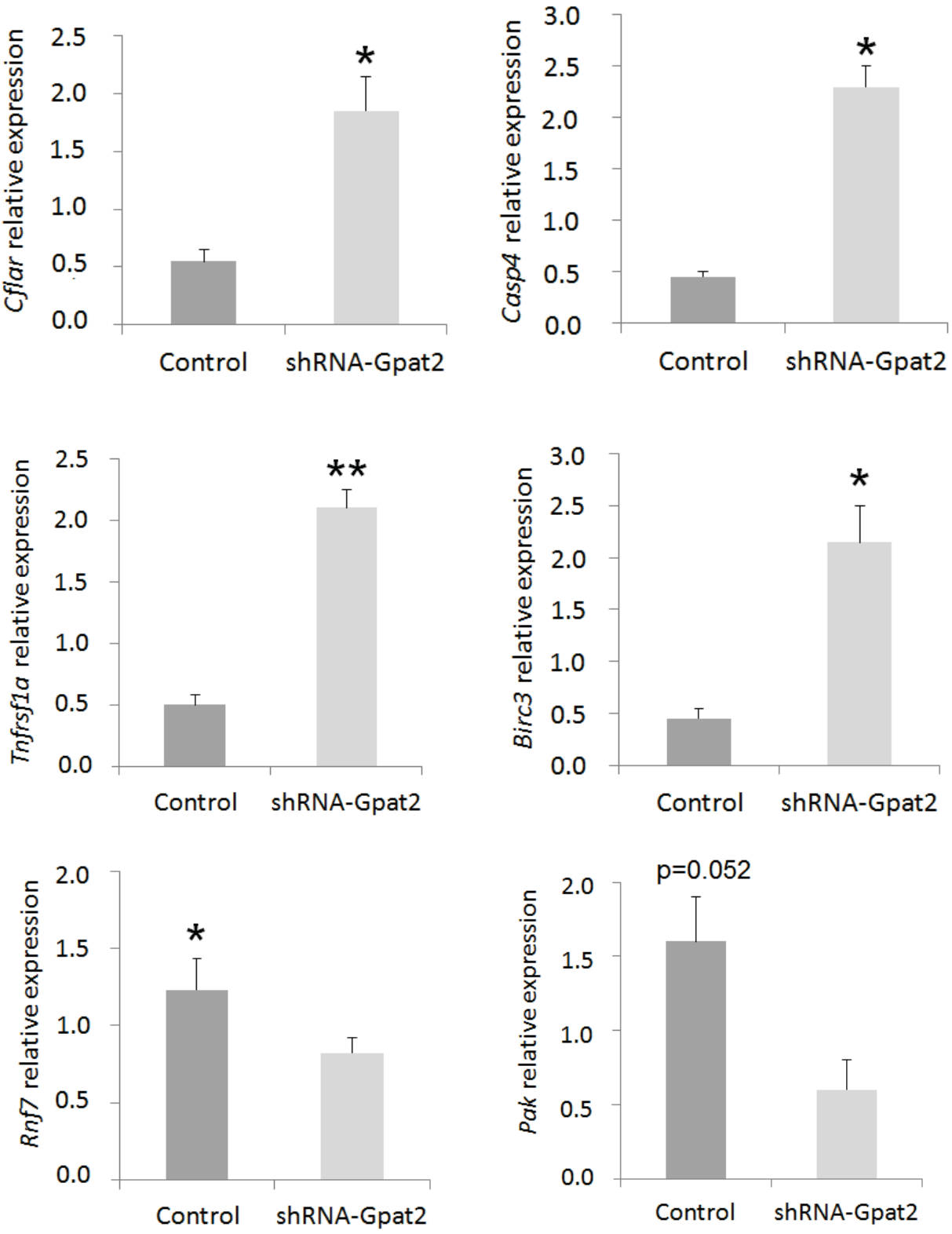
Cflar relative expression
2.5
2.0
1.5
1.0
0.5
0.0
*
Control
shRNA-Gpat2
Casp4 relative expression
3.0
2.5
2.0
1.5
1.0
0.5
0.0
*
Control
shRNA-Gpat2
Tnfrsf1a relative expression
2.5
2.0
1.5
1.0
0.5
0.0
**
Control
shRNA-Gpat2
Birc3 relative expression
3.0
2.5
2.0
1.5
1.0
0.5
0.0
*
Control
shRNA-Gpat2
Rnf7 relative expression
2.0
1.5
1.0
0.5
0.0
*
Control
shRNA-Gpat2
Pak relative expression
p=0.052
2.0
1.5
1.0
0.5
0.0
Control
shRNA-Gpat2

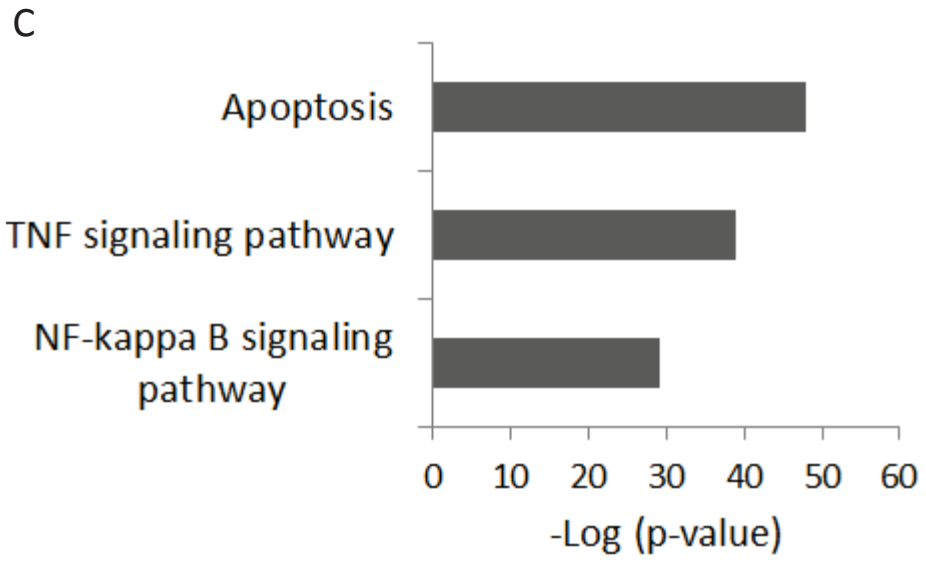

Figure 7. *Gpat2* silencing triggers the expression of apoptotic-related genes. Mice were inoculated with shRNA-*Gpat2* (n=7) or Control (n=5) lentiviral particles respectively. One month later germ cells were purified for RNA extraction. (A) Apoptosis-related genes were measured with RT2 Profiler Apoptosis Array and results are shown as the ratio between iRNA-*Gpat2*/SCR gene expression (FC). Only genes with a Log_2FC (LFC)>1 (12 genes) or LFC<-1 (2 genes) are shown. The number of upregulated genes is significantly higher than the downregulated ones ($p<0.001$, Chi-Square test), indicating a progression towards apoptosis in *Gpat2* silenced germ cells. (B) Six of the deregulated genes were confirmed by qPCR. Bars indicate the means ± SD of two independent experiments; * $p < 0.05$; ** $p < 0.01$ (Student's t test). (C) Functional analysis, according to gene ontology of upregulated genes with an FC≥ 1.3, revealed that TNF and NF-kappa beta apoptosis were the most affected pathways.

Supplementary Information

Table S1. Primers used in this study.

Gene	Primer sequence	
Gpat2	Forward	ATCCTACTGCTGCTGCACCT
	Reverse	ACAGCAGCTTTGCACTCAGA
Nanos3	Forward	TTCTGCAGGCAAAAAGCTGAC
	Reverse	TTTTGGAACCTGCATAGACACC
Tmem30c	Forward	TACCTTCCGGAGAAAATGGAG
	Reverse	TCACAGTTCGTAGTATCCCAAATA
Tpn1	Forward	AGCCGCAAGCTAAAGACTCA
	Reverse	TTGCGACTTGCATCATCGCC
L15UTR	Forward	GGCGAAAGGCAAACGTAAGA
	Reverse	GGAGTGCTGCGTTCTGATGA
L1ORF2	Forward	GGAGGGACATTTCATTCTCATCA
	Reverse	GCTGCTCTTGTATTTGGAGCATAGA
IAP3LTR	Forward	GCACATGCGCAGATTATTTGTT
	Reverse	CCACATTCGCCGTTACAAGAT
IAPGag	Forward	AACCAATGCTAATTTCACCTTGGT
	Reverse	GCCAATCAGCAGGCGTTAGT
Casp4	Forward	AACCCCACATCACTTGTCCT
	Reverse	GGTGGGCATCTGGGAATGAA
Cflar	Forward	GGCAGAGGCAAGATAGCCAA
	Reverse	ATCTTGCTCCTTGGCTGGAC
Tnfrsf1a	Forward	CACCGTGACAATCCCCTGTAA
	Reverse	TTTGCAAGCGGAGGAGGTAG
Rnf7	Forward	TCCAGGTGATGGATGCCTGC
	Reverse	AGAGGGCAGCGATTGTTCTG
Pak7	Forward	AGCGATGGCCGGATAAAGTT
	Reverse	GGGGCTCCCCATCAATCATC
Birc3	Forward	TGCCAAGTGGTTTCCAAGGT
	Reverse	CAAAATGCACGATTGCTGCG
Rpl13A	Forward	ATGACAAGAAAAAGCGGATG
	Reverse	CTTTTCTGCCTGTTTCCGTA
***TBP* (Homo sapiens)**	Forward	TATAATCCCAAGCGGTTTGC
	Reverse	GCTGGAAAACCCAACTTCTG

Table S1. Sequences of primers used in this study. All but *TBP* have been designed against *Mus musculus*. L15UTR, L1ORF2, IAP3LTR and IAPGag primer sequences were obtained from [1].

Table S2. shRNA-*Gpat2* sequences.

Clone	Identification number	Sequence
1	V2LMM_105431	TGTACATTCAGGAAGAGGC
2	V3LMM_499833	TGAGGTAGCAGGTGCAGCA
3	V3LMM_499830	AGGTCTTGAGGTAGCAGGT
4	V3LMM_499834	TGAACGTCCAGACTGCACT
5	V3LMM_499835	ACAACACTACATTCACCTA

Table S2. shRNA-*Gpat2* sequences. These sequences form part of GIPZ Lentiviral shRNAmir vectors (Thermo Scientific), which encode a shRNA that targets different regions of mouse *Gpat2* mRNA. Each one was cotransfected with *Gpat2* expression vector (pcDNA3.1-Gpat2 [2]) into HEK 293 cell line in order to select the best silencing vector. *Gpat2* expression was evaluated by qPCR and the lowest expression was achieved with the clone N° 4 (Figure S1).

Figure S1. *Gpat2* silencing optimization and shRNA selection.

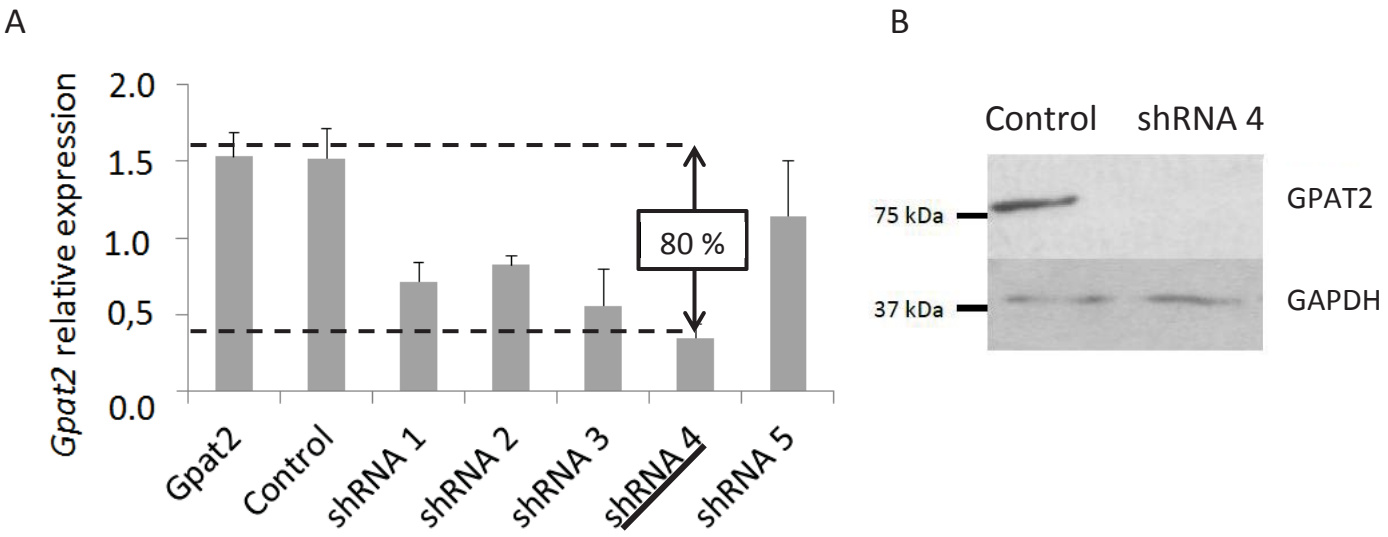

Figure S1. *Gpat2* silencing optimization. (A) shRNA vectors were cotransfected with a *Gpat2* expression vector in HEK 293 cells and 48 hours later *Gpat2* relative expression was evaluated by qPCR, using human *TBP* as an internal control. All but the "Gpat2" sample were cotransfected with *Gpat2* expression vector and the Control vector (with a scrambled sequence) or shRNA vector. The mean ± SD from two independent experiments are shown. The most effective silencing vector was shRNA 4, reaching a reduction of 80 % in *Gpat2* expression in comparison to Gpat2 or Control samples. (B) Protein descent was confirmed by Western blot in total cellular homogenate after vector cotransfection.

Figure S2. Testicular inoculation optimization.

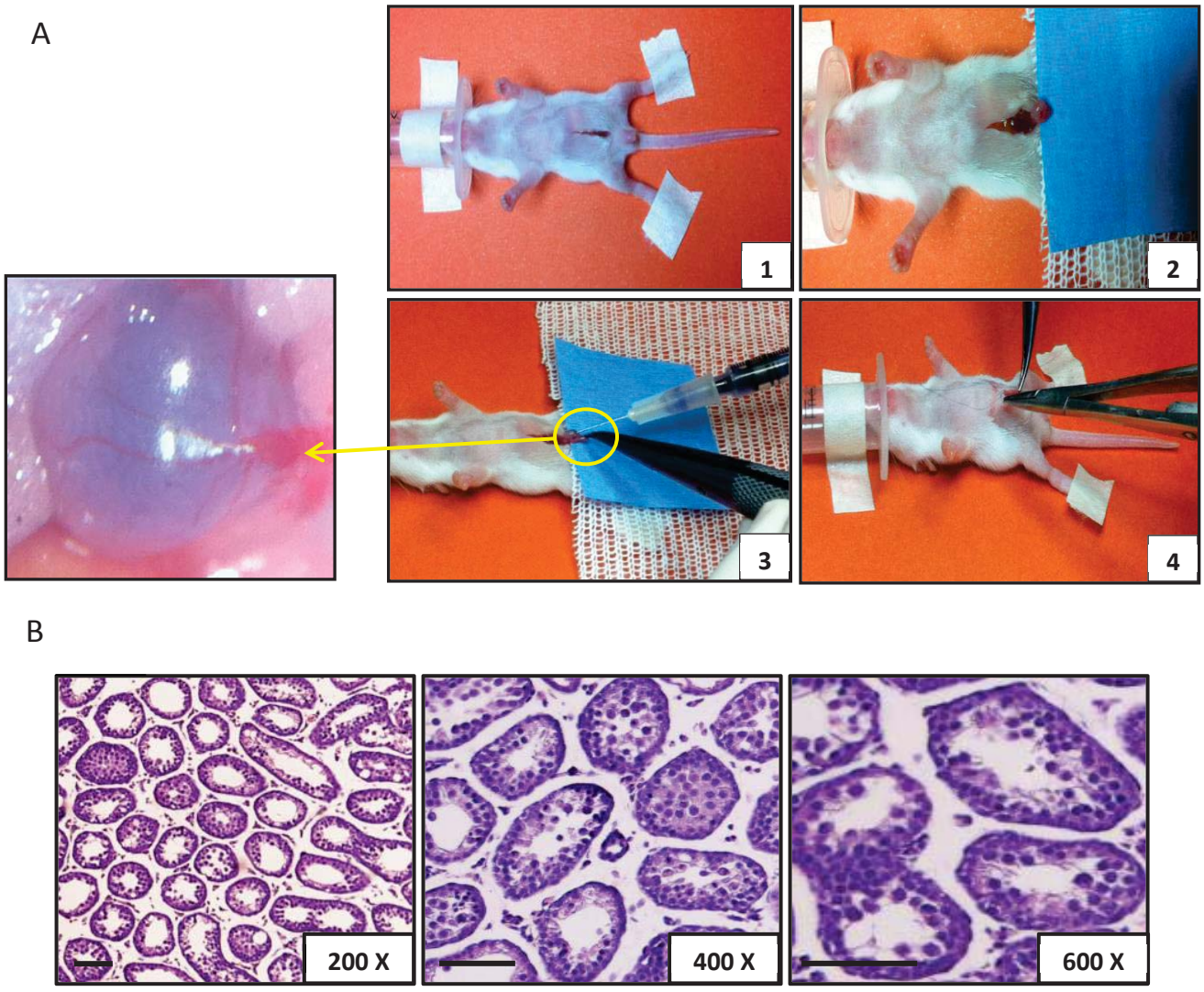

Figure S2. Testicular inoculation optimization in 11 dpp mice. (A) Four mice were anesthetized with isoflurane 1 % in oxygen. Firstly, an incision in abdominal cavity was done (1), testes were pulled out from it (2), inoculation was done with a 30G needle (3) and finally, the abdominal cavity was closed with 8-0 Vicryl suture. Trypan blue was added to PBS in order to follow its penetration across seminiferous tubules (inserted image). (B) Ten days after testicular inoculation two mice were sacrificed, testes were removed, fixed in Bouin´s solution, 10 µM slides were cut and haematoxylin-eosin stain was performed. A normal histology of an immature testis (21 dpp) is observed. The other two animals were mated with two females each to test their reproductive fitness. We observed a normal reproductive behavior and capacity, since the litter size and the latency for the first litter was statistically equal in comparison to the control mice (not inoculated, not shown). Magnifications are indicated in the lower right corner. Scale bars: 50 µM.

Figure S3. Testis size after *Gpat2* silencing

Figure S3. Testis size after *Gpat2* silencing. Representative photos of testis size are displayed. The yellow coloration is a consequence of the Bouin´s fixation solution. Although shRNA-*Gpat2* showed more variability in testis size than the Control group testes, no significant differences in their weight were observed between groups.

Figure S4. Vector maps.

A

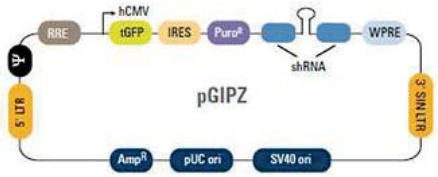

Vector Element	Utility
hCMV	Human cytomegalovirus promoter drives strong transgene expression
tGFP	TurboGFP reporter for visual tracking of transduction and expression
Puro^R	Puromycin resistance permits antibiotic-selective pressure and propagation of stable integrants
IRES	Internal ribosomal entry site allows expression of TurboGFP and puromycin resistance genes in a single transcript
shRNA	microRNA-adapted shRNA (based on miR-30) for gene knockdown
5' LTR	5' long terminal repeat
3' SIN LTR	3' self-inactivating long terminal repeat for increased lentivirus safety
Ψ	Psi packaging sequence allows viral genome packaging using lentiviral packaging systems
RRE	Rev response element enhances titer by increasing packaging efficiency of full-length viral genomes
WPRE	Woodchuck hepatitis posttranscriptional regulatory element enhances transgene expression in the target cells

B

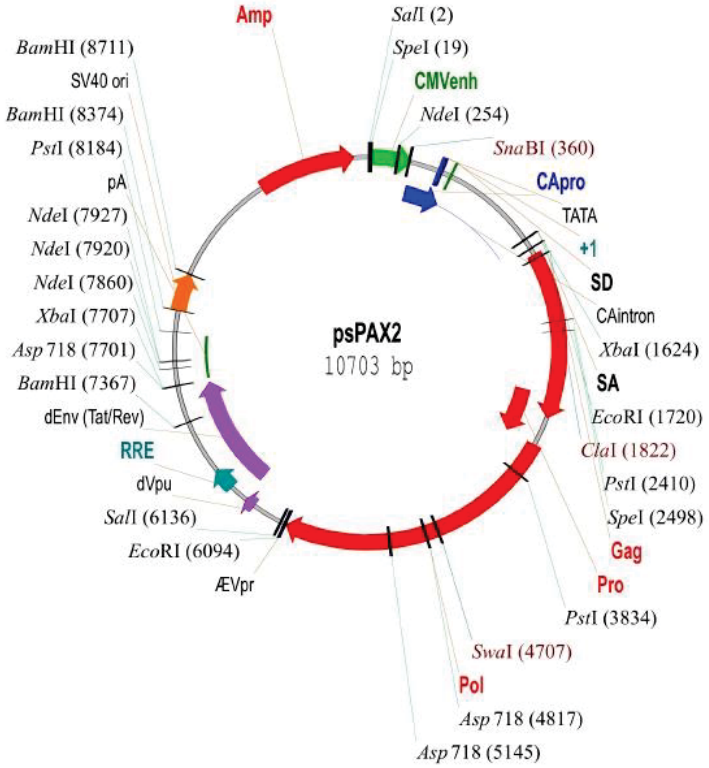

C

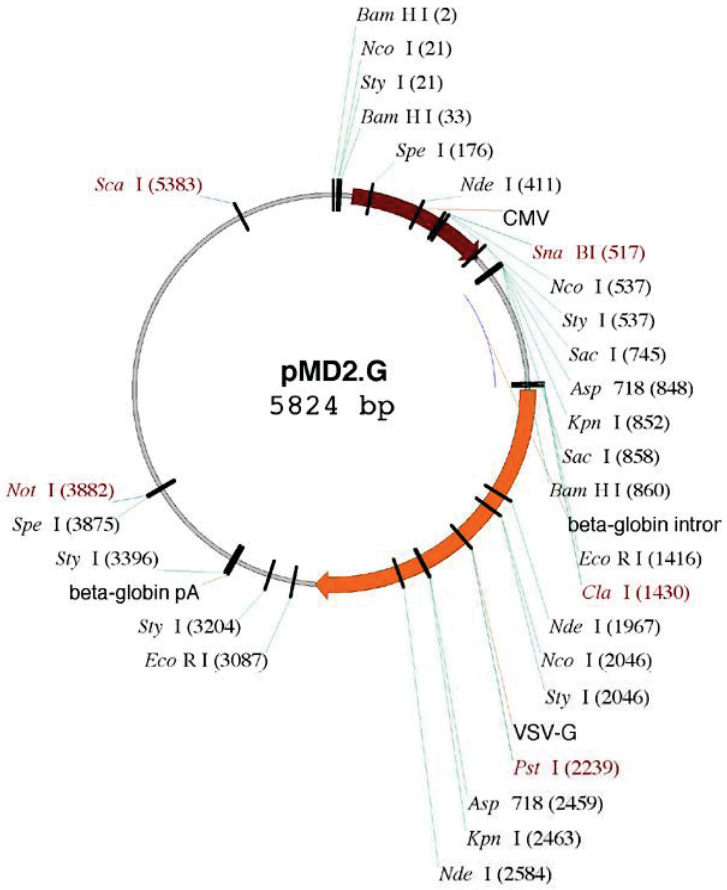

Figure S4. Vector maps of the vectors used for lentiviral production. (A) pGIPZ vectors encoding five different shRNA targeting *Gpat2* transcript (shRNA vectors) or a scrambled sequence (Control) were purchased from Thermo Scientific. (B) psPAX plasmid is the lentiviral packaging plasmid and (C) pMD2.G is the lentiviral envelope plasmid expressing VSV-G protein, which confers broad tropism over a range of species and cell type. Both vectors were purchased from Addgene.

Figure S5. TLC for total lipids from shRNA-*Gpat2* and Control testes.

A

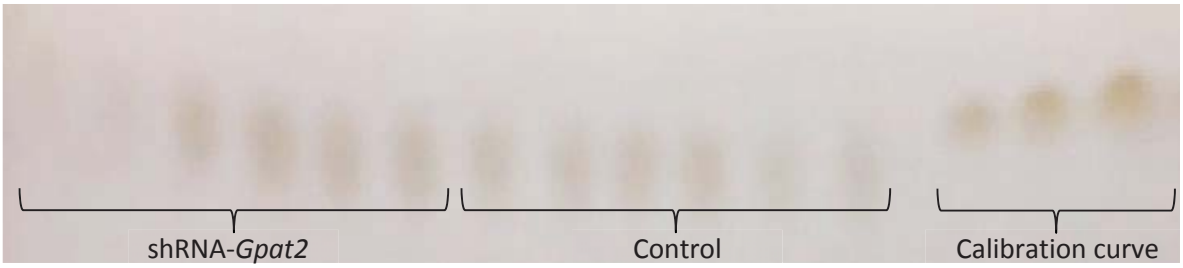

B

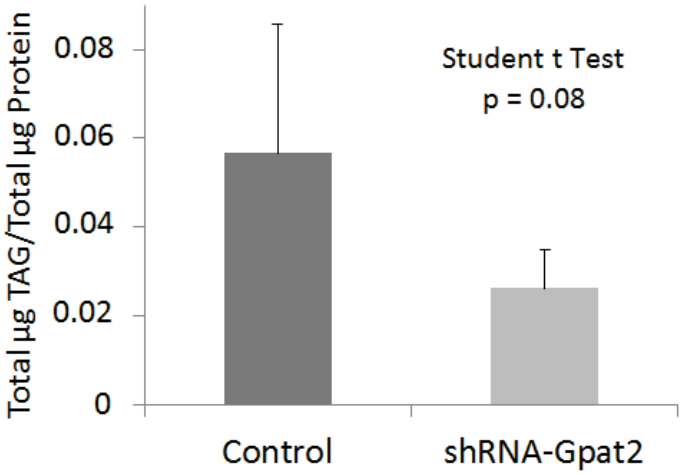

Figure S5. TLC for total lipids. (A) Ten µl of total lipid extracts were seeded in the bottom of the TLC plate and run for 50 min with a mobile phase composed of hexane-ethyl ether-acetic acid (80:20:2; v/v) for neutral lipids. (B) TLC plate was carbonized and analyzed with ImageJ software.

Table S3: Human *GPAT2* silencing in MDA-MB-231 cells did not affect total GPAT activity.

	Control cells	*GPAT2*-KD cells
Specific Activity (nmol/min/mg prot)	3.05 ± 0.21	3.16 ± 0.43

Table S3: GPAT activity was assayed as previously described [2]. GPAT2 was stably silenced in MDA-MB-231 cells as previously reported [3]. Data are expressed as mean ± SD of an experiment performed in triplicate. $p = 0.58$.

Figure S6. Intrinsically disordered regions predicted for the 4 isoforms of murine GPAT.

A

#	% LD	Entry ID	Length	Protein Name	Organism
1	0.000 %	Q8K2C8	456	Glycerol-3-phosphate acyltransferase 4	Mus musculus
2	02.87 %	Q14DK4	801	Glycerol-3-phosphate acyltransferase 2, mitochondrial	Mus musculus
3	0.000 %	Q61586	827	Glycerol-3-phosphate acyltransferase 1, mitochondrial	Mus musculus
4	0.000 %	Q8C0N2	438	Glycerol-3-phosphate acyltransferase 3	Mus musculus

B

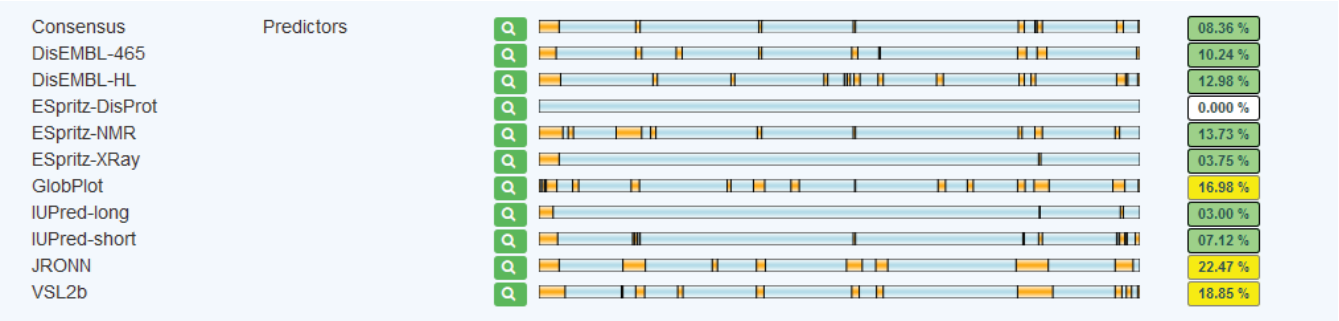

Figure S7. (A) Frequency of residues in long disordered regions (%LD) of the 4 known isoforms of mouse GPAT, as analyzed using MobiDB (http://mobidb.bio.unipd.it/). (B) Prediction of the disordered regions of murine GPAT2 (yellow blocks). The detailed information of each predictor used can be found at http://mobidb.bio.unipd.it/entries/Q14DK4.

Figure S7. Deregulated apoptosis-related genes

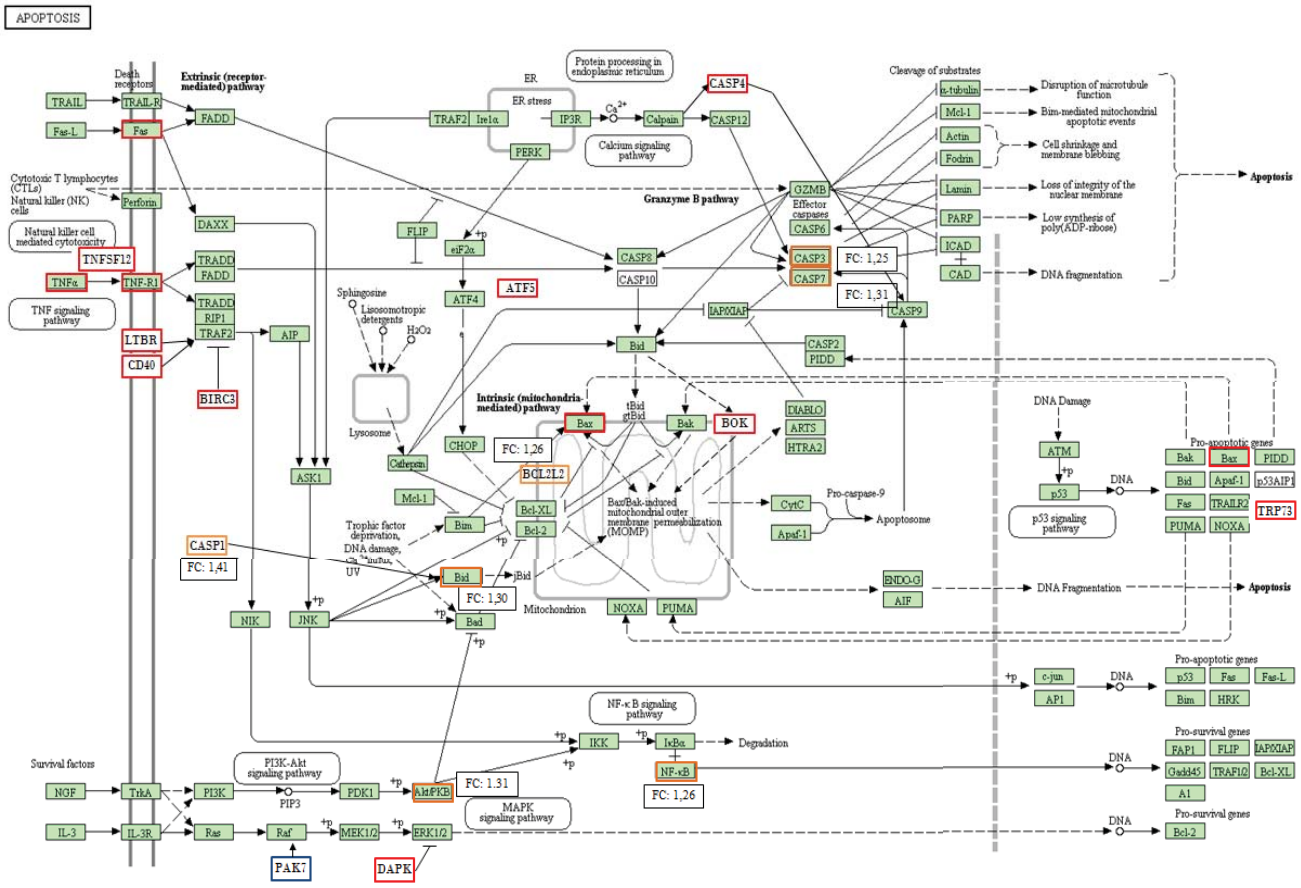

Figure S6. Apoptosis pathways showing deregulated genes in shRNA-*Gpat2* compared to Control germ cells. The apoptosis pathway scheme was obtained from KEGG 2016 database. Only those genes which are most related to apoptosis and which can be found in the pathways are shown. Upregulated genes in shRNA-*Gpat2* germ cells with a FC>1,5 (Log_2> 0,58) are indicated in red, upregulated genes in shRNA-*Gpat2* germ cells with a FC between 1,2-1,5 are indicated in orange and significantly downregulated genes are indicated in blue (FC<0,67 (1/1,5)).

References

1. Carmell MA, Girard A, van de Kant HJ, Bourc'his D, Bestor TH, et al. (2007) MIWI2 is essential for spermatogenesis and repression of transposons in the mouse male germline. Dev Cell 12: 503-514.
2. Cattaneo ER, Pellon-Maison M, Rabassa M, Lacunza E, Coleman RA and Gonzalez-Baro MR (2012) Glycerol-3-phosphate acyltransferase-2 is expressed in spermatic germ cells and incorporates arachidonic acid into triacylglycerols. PLoS One 7: e42986.

7. Pellon-Maison M, Montanaro MA, Lacunza E, Garcia-Fabiani MB, Soler-Gerino MC, Cattaneo ER, et al. Glycerol-3-phosphate acyltranferase-2 behaves as a cancer testis gene and promotes growth and tumorigenicity of the breast cancer MDA-MB-231 cell line. PloS one. 2014;9(6):e100896.